VYSOKÉ UČENÍ TECHNICKÉ V BRNĚ

CEITEC
Central European Institute of Technology
BRNO | CZECH REPUBLIC

BRNO UNIVERSITY OF TECHNOLOGY

VYSOKÉ UČENÍ TECHNICKÉ V BRNĚ

CENTRAL EUROPEAN INSTITUTE OF TECHNOLOGY BUT

STŘEDOEVROPSKÝ TECHNOLOGICKÝ INSTITUT VUT

STUDY OF THE SYNTHESIS AND PROCESSING CONDITIONS ON THE STRUCTURE AND PROPERTIES OF (Ba, Ca) (Ti, Zr) O_3 LEAD FREE CERAMICS

STUDIE SYNTÉZ A PŘÍPRAVY BEZOLOVNATÉ KERAMIKY (Ba, Ca) (Ti, Zr) O_3 V ZÁVISLOSTI NA STRUKTUŘE A VÝSLEDNÝCH VLASTNOSTÍ

SHORT VERSION OF DOCTORAL THESIS

ZKRÁCENÁ VERZE DIZERTAČNÍ PRÁCE

AUTHOR
AUTOR PRÁCE
Vijay Bijalwan

SUPERVISOR
VEDOUCÍ PRÁCE
Prof. (Dr.) Timothy W. Button

CO-SUPERVISOR
ŠKOLITEL SPECIALISTA
Dr. Pavel Tofel

BRNO 2018

Abstract

The lead free piezoelectric ceramic is a current topic of interest to replace lead based ceramics due to the demand of environmental protection and health concerns. Different materials have been discovered so far, including (K, Na) NbO_3 (KNN), (Bi, Na) TiO_3 (BNT), (Bi, Na) TiO_3 – $BaTiO_3$ (BNT-BT) etc. However, their piezoelectric properties are not fully comparable to the lead based ceramics (e.g. Lead zirconate titanate ((Pb Zr)TiO_3). To match the high functional properties of Pb-based materials, a new material system, (1-x)$Ba(Zr_{0.2}Ti_{0.8})O_3$-x$(Ba_{0.7}Ca_{0.3})TiO_3$ or (Ba, Ca) (Zr, Ti) O_3 ((1-x)BZT-xBCT or BCZT) was recently found, which possess very high piezoelectric and dielectric properties. The drawback of this composition is its very high sintering temperature (1520°C) in order to achieve high piezoelectric properties (e.g. Piezoelectric constant d_{33} > 600 pC/N). In this work, based on BCZT system, ceramics with high functional properties were fabricated by addition/substitution of CeO_2 while reducing its sintering temperature to 1350°C.

The CeO_2 addition (y = 0.07 wt.%) to $(Ba_{0.85}Ca_{0.15})$ $(Zr_{0.1}Ti_{0.9})$ O_3 ceramic reduced its sintering temperature drastically and high densification was achieved at 1350°C, together with increased Curie Temperature, T_C ~ 105°C, and controlled grain size ~ 10 - 13 µm. The phase transition from rhombohedral to tetragonal (R-T) was identified between y = 0 - 0.1 wt.% by the X ray diffraction (XRD) which in line with the Raman spectra analysis. A detailed study of microstructural and structural characteristics is shown with its correlation to the dielectric, ferroelectric and piezoelectric properties. Best functional properties were observed for BCZT - y wt.% CeO_2 ceramics where y=0.07 wt.%, in which *piezoelectric constant* d_{33} = 507±20pC/N, *planar coupling coefficient* k_p = 51.8 %, *dielectric permittivity* ε_r = 4091±100, *tangent loss tan* δ = 0.02, *remenant polarization* P_r = 13.58µC/cm², *coercive field* E_C = 2.13kV/cm *and normalized strain* d_{33}^* *or* S_{max}/E_{max} = 840pm/V. The two step sintering (TSS) technique demonstrated a homogeneous grain growth and high density (~ 99% of theoretical density).

$(Ba_{0.85}Ca_{0.15-y}Ce_y)$ $(Zr_{0.1}Ti_{0.9})$ O_3 (BCCeZT) lead free piezoelectric ceramics were also prepared where CeO_2 was used as a substitution at A-site of BCZT's lattice system. The shifting of XRD peaks towards higher angles suggests cell contraction and we speculate occupation of Ce ions at A site. It is found that ~ (10 - 12) µm grain size is critical for the processing of high performance lead free BCCeZT ceramics. The best properties were obtained for y;Ce = 0.00135 sintered at 1350°C/4h having as d_{33} = 501±10 pC/N, k_p = 38.5±1.92 %, P_r = 12.19 µC/cm², T_C = 108.1 °C and *strain (S)* of 0.14 %. To investigate further the effects of A-site substitution, $(Ba_{1-x-y}Ca_xCe_y)$ $(Zr_{0.1}Ti_{0.9})$ O_3 ceramics (x:Ca = 0.05, 0.10, 0.15, 0.20 and y;Ce = 0.00135) were fabricated. Again, when grain size was ~ 13um, high piezoelectric properties (d_{33} = 457pC/N) for x;Ca = 0.15 were observed when sintered at 1425 °C, while when grain size > 16 microns, d_{33} reduced below 200 pC/N. the XRD analysis shows the phase transition from orthorhombic to tetragonal as x;Ca content increases. Finally, $(Ba_{0.85}Ca_{0.15})$ $(Zr_wCe_yTi_{1-w-y})$ O_3 ceramics were prepared where CeO_2 was used as a substitution at the B-site of BCZT's lattice system. XRD analysis shows a coexistence of tetragonal-orthorhombic phases for Zr (w) = 0.1 and Ce (y) = 0.00135. Temperature dependent dielectric properties show that as the Zr content

increases up to w;Zr = 0.1, the T_{O-T} and T_{R-O} peaks appeared. Excess Zr content (w > 0.1) shifts the T_{T-C} peak to very low temperatures that may affect the functional properties.

Abstrakt

V poslední době je snahou nahradit klasickou komerční olovnatou piezoelektrickou keramiku bezolovnatou, z důvodu zvýšeného zájmu o ochranu životního prostředí a zdraví. Různé typy materiálů již byly navrženy, jako například (K, Na) NbO_3 (KNN), (Bi, Na) TiO_3 (BNT), (Bi, Na) TiO_3 – $BaTiO_3$ (BNT-BT), ale jejich piezoelektrické vlastnosti zatím nedosáhly takových hodnot jako u olovnatý chkeramik (např. olovnatý titanát olova ((Pb Zr)TiO_3). Nejvíce se olovnatým materiálů blíží bezolovnatý systém na bázi (1-x)Ba($Zr_{0.2}Ti_{0.8}$)O_3-x($Ba_{0.7}Ca_{0.3}$)TiO_3 nebo (Ba, Ca) (Zr, Ti) O_3 ((1-x)BZT-xBCT, BCZT) a to díky vysokým piezoelektrickým a dielektrickým parametrům. Nevýhodou tohoto prostředku je jeho velmi vysoká teplota slinování (1520 ° C) za účelem dosažení vysokých piezoelektrických vlastností (např. Piezoelektrické konstanty d_{33} > 600 pC / N). Tato práce se zabývá bezolovnatou keramikou na bázi BCZT, její výrobou a vylepšením piezoelektrických vlastností dopováním CeO2.
Přidáním CeO_2 (y wt.%) do ($Ba_{0.85}Ca_{0.15}$) ($Zr_{0.1}T_{io.9}$) O_3 se výrazně snížila slinovací teplota a došlo ke zhutnění při 1350°C. U této kompozice se Curieova teplota pohybovala kolem T_C~105°C a velikost zrn byla v rozmezí ~ 10-13 μm. Fázový přechod z romboedrické struktury na tetragonální (R-T) byl zjištěn pomocí rentgenové spektroskopie u y = 0 - 0.1 wt.%, což koreluje s výsledky Ramanovy spektrální analýzy. Mikrostrukturní a strukturní charakteristiky byly detailně studovány v korelaci s dielektrickými, feroelektrickými a piezoelektrickými vlastnostmi. Nejlepší funkční vlastnosti byly dosaženy pro keramiku BCZT – 0.07 wt.% CeO_2. Tato keramika vykazovala piezoelektrický nábojový koeficient d_{33} = 507±20pC/N, elektromechanický planární koeficient k_p = 51.8 %, dielektrickou konstantu ε_r = 4091±100, ztrátový činitel $tan\ \delta$ = 0.02, remanentní polarizaci P_r = 13.58μC/cm², intenzitu koercitivního pole E_C = 2.13kV/cm při normovaném napětí, d_{33}* nebo S_{max}/E_{max} = 840pm/V. Dvoustupňovou kalcinační technikou bylo docíleno homogenního růstu zrn s vysokou relativní hustotou (~ 99% teoretické hustoty). Tato kompozice BCZT- CeO_2 vykazovala stálé feroelektrické, dielektrické a piezoelektrické vlastností i při velikosti zrn 10 μm.

Bezolovnatá piezoelektrická keramika ($Ba_{0.85}Ca_{0.15-y}Ce_y$) ($Zr_{0.1}T_{io.9}$) O_3 (BCCeZT) byla dále dopována CeO_2 s cílem substituce Ce^{4+} v místě A krystalické mřížky. Posunutí rentgenových vrcholů k vyšším úhlům naznačuje kontrakce mřížky, což by mohlo způsobit obsazení iontů ceru v místech A této soustavy. Bylo zjištěno, že velikost zrn kolem 10 - 12 μm je významná pro vysokou piezoaktivitu bezolovnaté BCCeZT keramiky. Nejvyšší piezoelektrické vlastnosti tato keramika vykazovala při y;Ce = 0.00135 a slinovaná na teplotě 1350°C/4h, kdy piezoelektrické parametry byly d_{33} = 501±10 pC/N, k_p = 38.5±1.92 %, P_r = 12.19 μC/cm², T_C = 108.1 °C a s maximální deformací S do 0.14 %. Pro další studium substituce v místě A, byly vyrobeny keramické materiály (Ba_{1-x-y} Ca_x Ce_y) ($Zr_{0.1}$ $Ti_{0.9}$) O_3 (x:Ca = 0.05, 0.10, 0.15, 0.20 a y;Ce = 0.00135). Opět se ukázalo, že pokud byla velikost zrn ~13um, tak keramika vykazovala vysoké piezoelektrické vlastnosti (d_{33} = 457pC/N) pro x = 0.15 % kalcinované na teplotě 1425 °C. Když se se velikost zrn zvýšila nad 16 um, piezoelektrický nábojový koeficient d_{33} klesl na 200 pC/N. Rentgenová analýza ukázala změnu fázové struktury z rombické

na tetragonální při zvýšení obsahu vápníku. Jako poslední byly připraveny keramiky ($Ba_{0.85}$ $Ca_{0.15}$) (Zr_w Ce_y Ti_{1-w-y}) O_3, kde CeO_2 bylo použito jako substituce na straně B krystalické mřížky. Rentgenová analýza ukázala koexistenci tetragonal-ortorombické faze pro Zr (w) = 0.1 and Ce (y) = 0.00135. Měřením dielektrických vlastností v závislosti na teplotě bylo zjištěno, že když obsah zirkonia stoupá až do w;Zr = 0.1, objevují se vrcholy T_{O-T} a $T_{R-O.}$ S dalším zvýšením obsahu zirkonia (w > 0.1) se vrcholy T_{T-C} posunuly k nižším teplotám, což může ovlivnit funkční vlastnosti materiálu.

Keywords:
Lead free ceramics, BCZT, Sintering, Grain size, CeO_2, Microstructure, Functional properties.

Klíčová Slova
Bezolovnatá keramika, BCZT, Sintra, Velikost zrna, CeO2, Mikrostruktura, Funkční vlastnosti.

Biblographic Citation
Bijalwan, V. Study of the synthesis and processing conditions on the structure and properties of (Ba, Ca) (Ti, Zr) O_3 lead free ceramics. Brno: Brno University of Technology, Central European Institute of Technology, 2018. 49 p. Dissertation supervisor: Prof. (Dr.) Timothy W. Button.

Biblografická Citace
Bijalwan, V. Studie syntéz a přípravy bezolovnaté keramiky (Ba, Ca) (Ti, Tr) O_3 v závislosti na struktuře a výsledných vlastností. Brno: Vysoké učení technické v Brně, Středoevropský technologický institut, 2018. 48 p. Vedoucí disertační práce: Prof. (Dr.) Timothy W. Button.

CEITEC BUT, Brno University of Technology, Czech Republic
Purkyňova 648/125, 621 00 Brno, Czech Republic
Vijay.bijawan@ceitec.vutbr.cz

Acknowledgements

First, I would like to express my deep sense of gratitude to my thesis supervisor Prof. Tim Button for offering me an opportunity to do research in ceramic laboratory in Central European Institute of Technology (CEITEC) Brno, Czech Republic and University of Birmingham UK. I gratefully acknowledge Prof. Tim Button for his kind support, excellent supervision, precise guidance during my PhD and his patience of reading and correcting my thesis. Then I would like to thank my thesis co-supervisor Dr. Pavel Tofel for his constant support and suggestions during my research specially while obtaining experimental results on different equipment's as well as helping me out when I was uncomfortable and ill.

My special thanks to Dr. Hana Hughes and Dr. Yang Bai for giving me a helping hand in my experimental work in University of Birmingham, UK and CEITEC, Brno University of Technology, Czech Republic. Apart from that, I will never forget the barbeque parties at Hana's house with all our colleagues and friends was truly amazing.

I would like to sincerely acknowledge the support and important guidance from Prof. (Dr.) Karel Maca during my entire PhD study which help me understand the key parameters of sintering techniques and overall ceramic processing parameters.

Special thanks to Prof. Martín Trunec, Dr. Klára Častková, Prof. Jaroslav Cihlář and Prof. Jiří Erhart for their useful suggestions of solving technical problems.

I would like to express my gratitude to Mr. Carl Meggs for his professional training on the laboratory equipment and practical advice on the experimental design in University of Birmingham, UK.

My heartiest thanks to office colleagues Hojat pooladvand, Tanikan, at University of Birmingham and CEITEC laboratory colleagues Bo Nan, Hua Tan, Vaclav Pouchly, Martín Kachlík, Jaroslav Kaštyl for their useful suggestions about my experimental work. The gratitude belongs to the entire advanced ceramic group, CEITEC, Brno university of technology.

I deeply acknowledge CEITEC PhD scholarship and Erasmus plus program funding for covering up all my study and living costs in Brno, Czech Republic and Birmingham UK.

Special thanks to my parents for their constant support without which it would have not been possible.

Finally, I would like to dedicate this thesis to my family. It's been tough years living far from you. Thanks a lot for your love, trust and support.

Sworn Statement

I hereby declare that I have written the PhD thesis on my own according to advice of my supervisor prof. Dr. Timothy. W. Button and that all the literary sources are quoted correctly and completely. This dissertation thesis is the property of the Central European Institute of Technology (CEITEC), Brno University of Technology (BUT), Czech Republic and it can be used for commercial purposes only with consent of the doctoral thesis supervisor and the director of CEITEC, BUT.

Čestné prohlášení

Tímto prohlašuji, že jsem vypracoval doktorskou práci sám, dle doporučení vedoucího prof. Dr. Timothy. W. Buttona a že všechny literární zdroje jsou citovány správně a úplně. Tato disertační práce je majetkem Středoevropského technologického institutu (CEITEC), VUT v Brně a může být použita ke komerčním účelům pouze se souhlasem vedoucího disertační práce a ředitele CEITEC VUT v Brně .

Vijay Bijalwan

Contents

1. Introduction

About ten years back Saito et.al. [1] had spurned wide-spread scientific activity in finding to replace lead based piezo ceramics dominated by Pb (Zr,Ti) O_3 abbreviated as PZT from with non-poisonous options. As a result, the legislative activity by the European Union [2-4] prepared to vanish toxic substances from industrial and household equipment's to eliminate their impact on environment and health. This particular work got wide attention for finding a combination of morphotropic phase boundary and polymorphic phase transition in a (K, Na) NbO_3 (KNN)- based lead-free system with similar piezoelectric properties like PZT.

The lead free piezoelectric ceramics is a broad term that contains basically two general groups. Out of which one group competes for the similar applications as PZT and another deal with the properties that are outside the range of PZT applications. First group belongs to (K, Na, Nb) O_5, (Ba, Ca) (Zr, Ti) O_3 and (Bi, Na)TiO_3-$BaTiO_3$ [often abbreviated as KNN, BCZT and BNT-BT respectively] derived materials. Second group materials such as (Ba, Zr, Ti) O_3, (Bi, Na, K, Ti) O_3 etc, commonly abbreviated as BZT, and BNKT respectively, whose properties may be inferior to the PZT material systems. Piezoelectric ceramics commands a widespread market as well as acting as an enabling technology for different areas, for example in photolithography (microelectronics through positioning elements), ultrasound imaging (medical diagnostics), sensors and actuators, and so on [5]. Some particular areas like domain wall properties relations of microstructures have been reviewed by Damjanovic [6], on the other hand publication by Shrout and Zhang [7] differentiate PZT with lead free piezoceramics, while Li et al. [8] summarized KNN-based materials. A publication by Rödel et al. [9] describes the precautions while dealing with electronic structure, important elements, also the phase diagrams. There are some other reviews that put light on the effects of different doping element on electrical properties [10], while crystallographic feature was well summarized by Aksel and Jones [11]. Now research is being saturated in KNN and BNT-based materials, but relatively new $Ba_{0.85}Ca_{0.15}Ti_{0.9}Zr_{0.1}O_3$, (BCZT) system has open the doors for the investigation of lead free piezoelectric ceramics due to its high piezoelectric properties (d_{33} = 620 pC/N) and shows similar kind of morphotropic phase boundary (MPB) as PZT does [12]. There are some drawbacks of this composition that includes low curie temperature (T_C ~ 95°C) and large grain growth due to its very high sintering temperature (>1500°C). Thus, lot of efforts has been done by researchers to lower its sintering temperature in order to obtain small grain size for technological applications. A research work [13] shows reduced processing and sintering temperature and low grain size while maintaining good piezoelectric properties (d_{33} > 400 pC/N). Other work including MnO-BCZT [14] and CeO_2-BCZT [15] has been done on reducing its sintering temperature.

Although lead free piezoelectric ceramic such as BCZT has most properties comparable to PZT but despite that it is far inferior from the everyday applications due to the high processing and sintering temperature as well as large grain size reduces its possibility to miniaturization. Therefore, the main idea of this thesis is to study and understand the full structural change of BCZT with and without dopant, and thereafter achieve optimized composition (low sintering temperature) with small grain size which could be potentially use in order to model and design lead free piezoelectric devices.

2. Aims of doctoral thesis

The overall aim of this thesis is to carry out a systematic investigation of the synthesis and processing conditions of lead free piezoelectric ceramic materials on the basis of existing issues, challenges and most recent status in the field of piezoelectric ceramics. The new material system $(Ba,Ca)(Zr,Ti)O_3$ (BCZT) has been selected. The work will include a study of the fabrication and processing conditions and related characterization, in order to identify processing routes for materials to be used in different technological applications.
The main objectives can be outlined as follows.

- Synthesis of lead free BCZT bulk piezoelectric ceramics and optimization of the processing conditions.
- To study the effect of cerium oxide (CeO_2) as an additive in the range (0 wt. % - 3 wt. %) on the structure and properties of BCZT and to elucidate the effect on sintering temperature and grain growth.
- To fabricate and characterize (Ba, Ca) - Ce - (Zr, Ti) O_3 ceramics (where Ce is a substitution on both the the A and B sites) and compare with the results for Ce as an additive.
- Correlation between structure, microstructure, grain size and functional properties was demonstrated.
- Detailed study of the effect of CeO_2 on its dielectric, Piezoelectric and ferroelectric properties was demonstrated.

3. Processing and Characterization techniques

3.1 Bulk ceramic processing

The mixed oxide route/conventional method is the most common method to synthesize $(Ba_{0.85}Ca_{0.15})(Zr_{0.1}Ti_{0.9})O_3$ or BCZT ceramics. In this research CeO_2 was used as an additive as well as substitution at A site and B site of BCZT perovskite structure.

1. First experiment: pure BCZT powders was prepared and calcined then CeO_2 (y wt.%) mixed as an additive.
2. Second experiment: A site substitution of CeO_2, following ceramic system was prepared.
   (a) $(Ba_{0.85}Ca_{0.15-y}Ce_y)(Zr_{0.1}Ti_{0.9})O_3$ where, y = 0, 0.0008 mol., 0.00135 mol., 0.02 mol.
   (b) $(Ba_{1-x-y}Ca_xCe_y)(Zr_{0.1}Ti_{0.9})O_3$ where, x = 0.05 mol., 0.10 mol., 0.15 mol., 0.20mol and y = 0.00135)
3. Third experiment: B site substitution of CeO_2, following ceramic system was prepared.
   (a) $(Ba_{0.85}Ca_{0.15})(Zr_wCe_yTi_{1-w-y})O_3$ where, x= 0 mol., 0.05 mol., 0.10 mol., 0.20 mol. and y = 0.00135 mol.

Oxide powders were used as raw materials to fabricate BCZT ceramics. The powders purity, particle size and manufacturers used in this research are presented in table 1.

Table 1. Component oxide powders used in synthesis of BCZT-CeO_2 ceramics.

Materials	Grade	Mean particle size(X_{50})	Manufacturer
$BaCO_3$	99.9 %	3.33±0.05 µm	Dakram, Great Britain
$CaCO_3$	99.9 %	47.37±0.05 µm	Lachner, Czech Republic
ZrO_2	99.9 %	2.80±0.05 µm	Dakram, Great Britain
TiO_2	99.9 %	2.66±0.05 µm	Dakram, Great Britain
CeO_2	99.9 %	1.61±0.1 µm	Sigma Aldrich, Great Britain

Starting powders were dried in the oven (Lenton MMD/0229, England) at 220 °C/1h before weighing to remove moisture which might agglomerate the particles during milling and lead to inaccurate stoichiometries. The raw powders were then mixed in a horizontal ball mill with zirconia milling media in deionized water for 24 hours. The weight ratio of powder to zirconia milling media was 2:1. The resulting slurry was dried in the oven at 90 °C for 15 hours and then calcined in a zirconia crucible using muffle furnace (Lenton, 5696, England) at 1250 °C for 2h with ramp up and ramp down temperature of 5 °C/min. Different amounts of CeO_2 were added (addition part) in 30 gm batches of the calcined BCZT powders and re-milled in deionized water for 24 hours. Approximately 5 wt. % of each binder, Duramax B1000 (Product No. 74821, Chesham Chemicals Ltd., UK), B1007 (Product No. 74823, Chesham Chemicals Ltd., UK) were added during the last hour of milling. The particle sizes were measured with the help of particle size analyzer (Gracell, Sympa Tec, Germany) and average particle size of all batches were ~ 2 micrometers after calcination and re-milling. After drying the resulting powders were sieved (300 microns, VWR, England) and pressed at 15.5 kN (Instron, 5507, England) into the green bodies using a 13-mm diameter cylindrical steel die (P.T. No. 3000, Specac, UK). The green bodies were sintered in the muffle furnace (Lenton, 5696, England) at different temperatures via conventional sintering and two step sintering methods. The sintering regime is represented in figure 1.

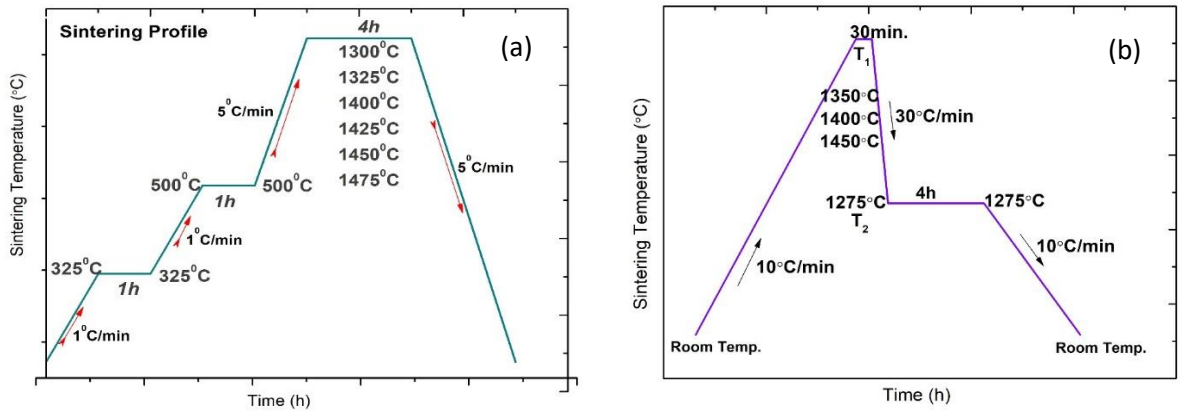

Fig. 1(a). Schematic of conventional sintering and (b) Two step sintering profile for BCZT-CeO_2 ceramics

3.2 Characterization

3.2.1 Density

The bulk density of the sintered discs/samples was obtained by calculating volume from the measured diameter and thickness dimensions ($V = \pi r^2 . t$) where r = radius = diameter/2 then divided that into the measured mass (M) in air. In this thesis, we assume that theoretical density of BCZT samples is 5.81 g/cm^3 which was previously reported [59].

3.2.2 Electrode Deposition and Poling

For all sintered discs, Chromium (Cr) – Gold (Au) electrodes were sputtered on the circular faces of the sintered samples using a sputter coater (K575X, Emitech, UK) to measure its dielectric properties. Before measuring piezoelectric properties, all the sintered samples were poled in silicone oil with an electric field of 3kV/mm for 10 min at room temperature. The fields were provided by a power supply (Alpha III, Brandenburg Ltd., UK).

3.2.3. X Ray diffraction and Scanning electron microscopy

The crystalline purity and phase structure of sintered discs was examined by X ray diffraction machine (SmartLab, Rigaku, Japan) Cu-Kα1 radiation (wavelength = 0.154 nm and diffraction angle (θ, $20° < 2\theta < 90°$), at room temperature. Powder diffraction file (PDF) ICDS #187673 was used for indexing the diffraction peaks obtained from the scanning.
The surface microstructure was observed by scanning electron microscopy (JEOL 6060LV, Japan) on surfaces which had been firstly polished, removing any fracture on the surface of the specimen, and thereafter thermally etched for 10 min at a temperature 100°C below the sintering temperature with ramp up and ramp down temperature as 20°C/min. Thermal etching is done to reveal the grain boundaries and then microstructural features such as grain size, grain size distribution, grain boundary and pores were characterized by using scanning electron microscope (SEM).

3.2.4. Raman spectroscopy

Raman spectra was recorded from Raman spectrometer (Renishaw InVia, UK) using a back scattered mode; the excitation laser was irradiated from an Ar^+ laser with an output power of 50mW. In Raman spectroscopy, sample is illuminated with a monochromatic laser beam which interacts with the molecules of sample and originates a scattered light. The scattered light having a frequency different from that of incident light (inelastic scattering) is used to construct a Raman spectrum.

3.2.5 Dielectric, piezoelectric and ferroelectric properties

The capacitance (labelled as C_S on the equipment) and dielectric loss factor ($tan\ \delta$) at 1 kHz were measured for all samples with an impedance analyser (4194A, Hewlett Packard, USA), at various

temperatures (-30 °C to 150 °C) with ramp up rate of 60 °C/hour controlled by an environmental chamber (TJR, Tenney Environmental-SPX, USA). The measured capacitances were calculated to corresponding relative permittivity ($\varepsilon_r = \varepsilon / \varepsilon_0$) where, $\varepsilon = C_s.t / r^2$ and $\varepsilon_o = 8.85 \times 10^{-12}$ F/m. Also, the resonant/anti-resonant frequencies (f_r, f_a) (Eq.1), were measured on another impedance analyzer (4294A, Agilent, USA) at room temperature which was used to calculate the electromechnical coupling coefficient/ planar coupling coefficient (k_p).
The piezoelectric charge coefficient (d_{33}) was directly measured on a quasi-static Berlincourt d_{33}-meter (YE2730A, Sinocera, China), where 5 random points of each sample were measured, and the average value was treated as the true d_{33}. This method is based on direct piezoelectric effect. The piezoelectric constant may have calculated from equation 2 where, Q is the induced charge (unit: pC or pico-coulomb) and F is force (unit: N or Newton) exerted on the sample along a particular direction. In practical sense, a Berlincourt d_{33} or d_{31} meter may directly measure the induced charge and applied force and hence calculated values are displayed on the equipment.

$$k_p^2 = 2.51 (f_a-f_r/f_r) - (f_a-f_r/f_r)^2 \quad (1)$$

and $$d_{ij} = \frac{Q}{F} \quad (2)$$

Ferroelectric characterization was carried out using the commercial aixACCT TF Analyzer 2000 test setup (aixACCT Systems GmbH, Germany) in combination with a TREK 20/20C (TREK, Inc., USA) high voltage amplifier. Initial electric characterization of bipolar electric field dependent large signal properties polarization P(E) and strain S(E) was performed on fresh samples. The large signal properties P(E) and S(E) were measured at a frequency of 1 Hz.

4. Selected Results and discussions

(I) Addition of CeO_2 (in y wt.%) to $(Ba_{0.85}Ca_{0.15})(Zr_{0.1}Ti_{0.9})O_3$ ceramics and sintered via conventional sintering.

4.1 Effects of sintering temperature on densities, microstructures and grain sizes

The bulk densities of BCZT ceramics with different Ce concentrations and sintered at various temperatures for 4 hours is depicted in figure 2. Generally speaking, bulk density increases with the increasing sintering temperature, however, samples with y = 0.04% and y = 0.07 % exhibit maximum density when sintered at 1350°C, with values of 5.57 g/cm^3 and 5.64 g/cm^3 respectively, corresponding to respective theoretical density values of nearly 95% and 97 % of the theoretical density of 5.81 g/cm^3 of 50/50 BCZT ceramics previously reported [16]. At higher sintering temperatures the density of samples with y = 0.04, 0.07, 0.1 and 3% CeO_2 either remain approximately constant or show a slight decrease, whereas for all other compositions the density continues to rise with increasing sintering temperature.

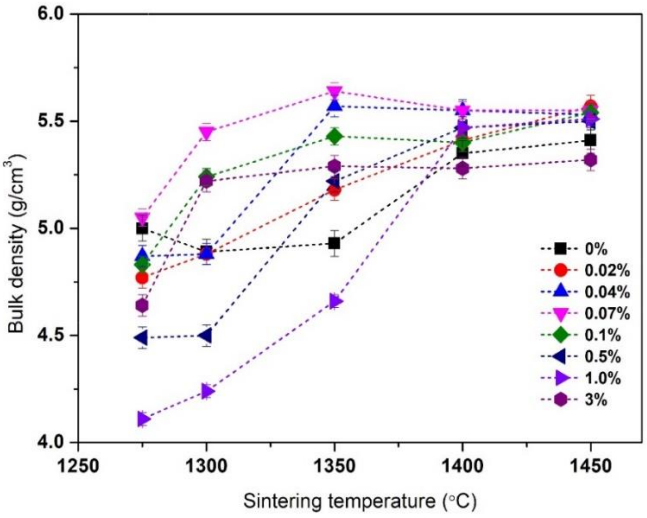

Fig. 2 Bulk density of BCZT-CeO_2 ceramics as a function of sintering temperature (4 hr)

The micrographs of BCZT - yCeO_2 ceramics sintered at 1350C° and 1450°C for 4 hours are shown in figure 3 (a-h), figure 4 (a-h) and the dependence of the average sintered grain size on sintering temperature is shown in figure 5. It is observed that the density of these samples is strongly dependent both upon their sintering temperature and composition. When sintered at 1350°C/4h (figure 3) the grain size increases for compositions in the range y = 0 - 0.1% and the addition of CeO_2 has caused a significant change in the grain size morphology and densification. For compositions in excess of y= 0.1% there seems almost no change in the morphology and density, indicating perhaps a saturation of the effect of the CeO_2 additive. Pure BCZT sintered at 1350°C (y = 0%, figure 3a) has an obvious porous microstructure. However, it is important to note that when y = 0.02% (Fig.3b) the microstructure has already started to become less porous. Samples with further incorporation of CeO_2 up to y = 0.04% (figure 3c) exhibit very dense microstructures with a number of large angular grains with small grains trapped between them. This abnormal grain growth implies a coarsening mechanism where a few large grains grow rapidly in a matrix of very small grains which have a much slower growth rate. In that sense, the microstructure can be considered to have a bimodal grain size distribution [17].

For samples in which the CeO_2 content was increased to y = 0.07% (figure 3d) a much more homogeneous grain structure is observed comprising primarily of large angular grains, with just a few finer grains and porosity at their junctions. It is well known that grain size, density and sintering temperature are very influential in obtaining high performance BCZT ceramics. For 50/50 BCZT, high density (> 95%) has been reported for ceramics sintered at temperatures >1500°C [12] with grain sizes greater than 30 μm [18]. In the present work we show that the addition of a small concentration of CeO_2 in the range y = 0.02 - 0.07% results in high densification (figure 2 & figure 3) for samples sintered at 1350°C, and results in average grain sizes of 10 - 13 μm (Fig.5). It is believed that the CeO_2 addition stimulates the mobility of grain boundaries that could potentially reduce the porosity at lower sintering temperatures [15].

However, it can be seen in figure 3 (e-g) that CeO_2 contents y = 0.1, 0.5, 1 and 3% result in porous microstructures, the x = 0.1% sample being a particular contrast to y = 0.07%. Here at low temperature small CeO_2 content (y = 0.02 - 0.07%) facilitates the grain growth of BCZT ceramics in contrast to reports for other lead free composition [19].

Figure 4 (a-h) show microstructures for BCZT-xCeO_2 ceramics sintered at 1450°C/4h. At this higher sintering temperature, grain growth is observed as the CeO_2 content is increased, with some porosity between the grains for the samples y = 0.04% and y = 0.07%. This small porosity at higher temperature could be achieved when grain growth is started before densification has been completed [18]. Similar to the samples sintered at 1350°C, there was no clear indication of microstructure evolution for the samples with composition y = 0.5, 3% even at this higher sintering temperature of 1450°C.

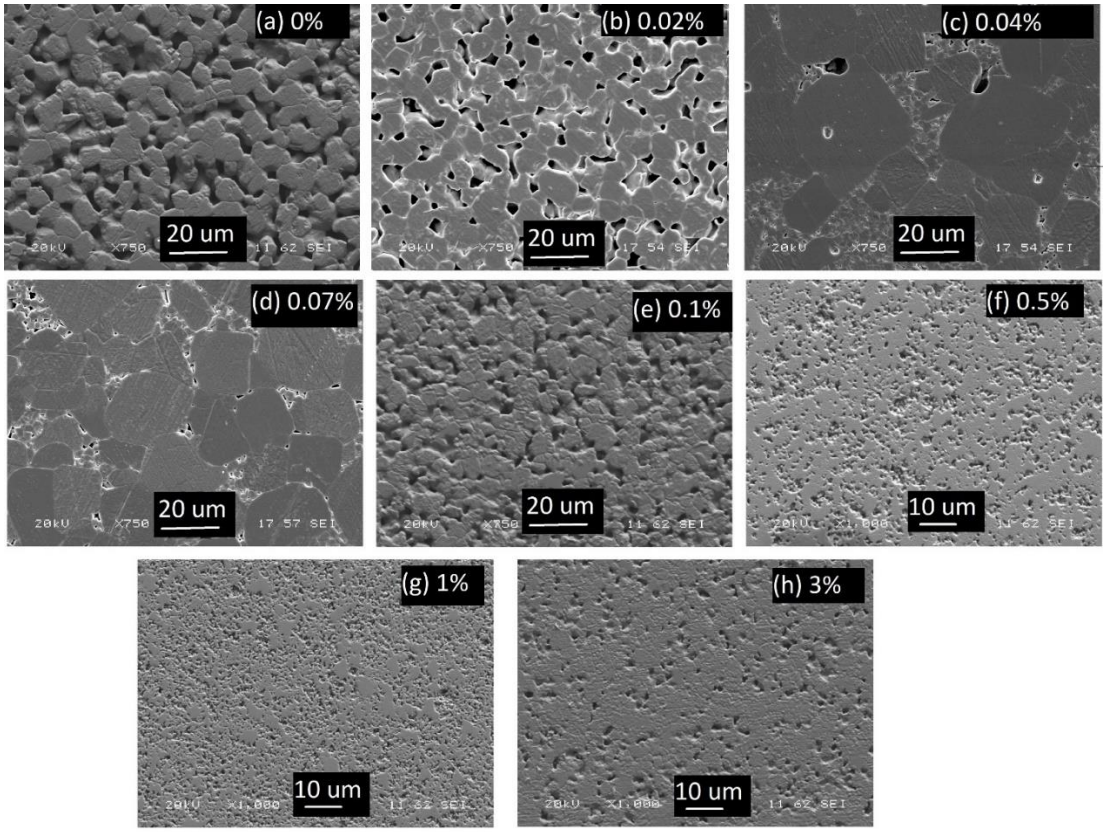

Fig. 3. SEM microstructures of BCZT - yCeO_2 samples for (a) y=0% (b) y=0.02% (c) y=0.04% (d) y=0.07% (e) y= 0.1% (f) 0.5% (g) y=1% (h) y=3% sintered at 1350°C for 4 hours.

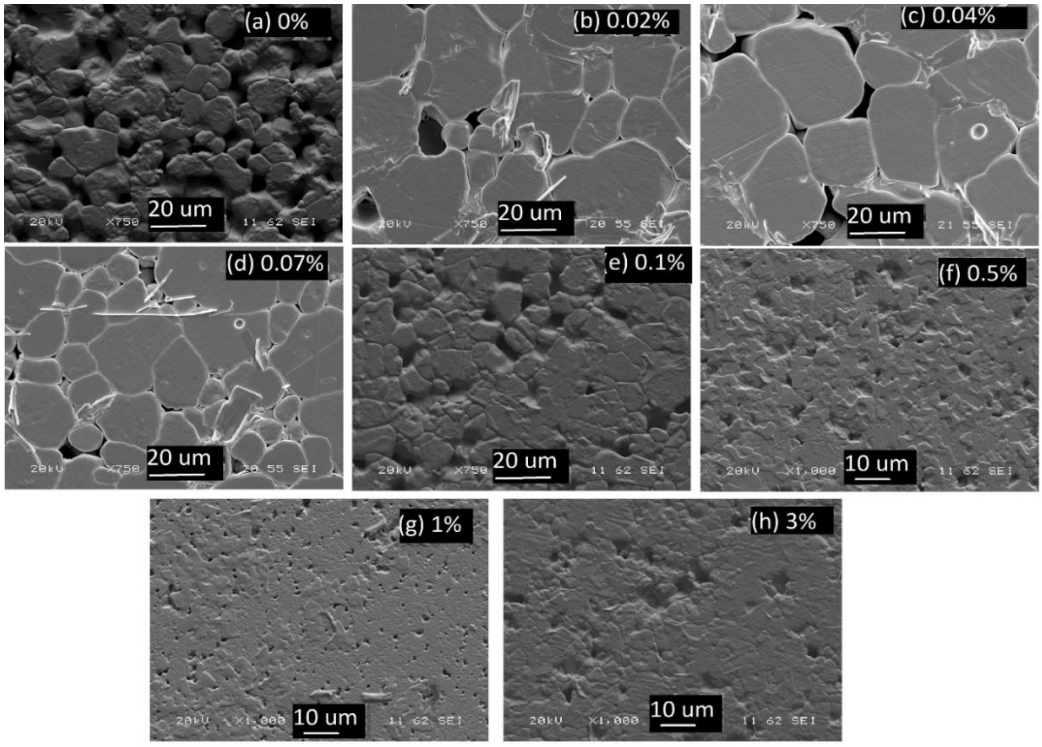

Fig. 4. SEM microstructures of BCZT - $yCeO_2$ samples for (a) y=0% (b) y=0.02% (c) y=0.04% (d) y=0.07% (e) y= 0.1% (f) y=0.5% (g) y=1% (h) y=3% sintered at 1450°C for 4 hours.

It is evident from the figure 5 that average grain size is very dependent on the sintering temperature, generally increasing as the sintering temperature is increased [18, 20].
At 1450°C the grains grow rapidly (>20 µm, figure 5) for compositions in the range y=0.02-0.07%. In addition, grain size is continuously increased for the sample y = 0%, as the temperature is increased up to 1450°C. On the other hand, grain sizes are very small for samples with compositions of y = 0.1, 0.5, 3% during entire sintering regime. It seems that higher amounts of CeO_2 could limit grain growth. Samples with composition y = 1% show anomalous behaviour which is discussed in more detail in later sections below.

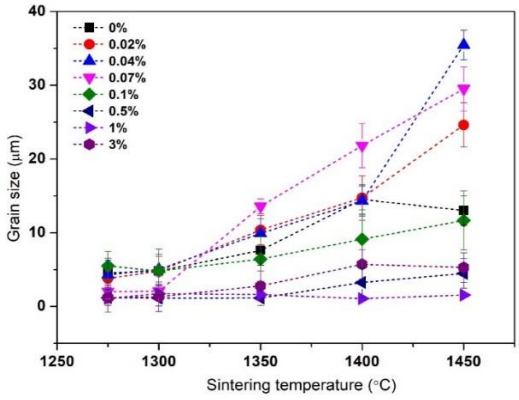

Fig. 5. Grain size dependence of BCZT - (0, 0.02, 0.04, 0.07, 0.1, 0.5, 1 and 3 % CeO_2) as a function of sintering temperature (4 hr).

4.2 Effects of sintering temperatures on piezoelectric properties.

The effect of sintering temperature on the piezoelectric charge constant d_{33} and planar coupling coefficient (k_p) for sintered BCZT samples with different amounts of CeO_2 are shown in figure 6(a) and 6(b) respectively. It can be seen that both properties generally increase with increased sintering temperature up to 1350°C. For samples with composition y=0.02-0.07, the values of d_{33} and k_p peak at this temperature, before decreasing with further increase in sintering temperature. For samples with compositions y= 0, 0.1, 0.5, and 3% CeO_2 the values of d_{33} and k_p increase further as the sintering temperature is increased beyond 1350°C, with values levelling off for some compositions at 1400°C. Again, the behaviour of the y=1.0% CeO_2 composition is anomalous, with very poor piezoelectric properties measured at all sintering temperatures. The maximum values of d_{33} and k_p were observed as 507±20 pC/N and 51.8% respectively for the y=0.07% composition sintered at 1350°C. These very high piezoelectric properties may be ascribed to the larger grain size (>10 micron) of BCZT ceramics facilitated by the CeO_2 addition. Also, samples with composition y > 0.07% sintered at 1350ºC exhibited inferior piezoelectric properties which may be attributed to the smaller grain sizes < 5 micron (see figure 5). Other reports confirm the appropriate grain size ~10-20 µm for obtaining high piezoelectric properties (d_{33}> 450pC/N) in BCZT [18, 20, 21]. Compared to pure BCZT (y=0%, grain size 7.6±2 µm) at 1350ºC the grain size has increased (10-15 µm) due to small amount of Ce content (y=0.02-0.07 %) which causes relatively high piezoelectric activity. There is also an indication from the data presented here that grain sizes larger than approximately 20µm may be deleterious to the piezoelectric properties.

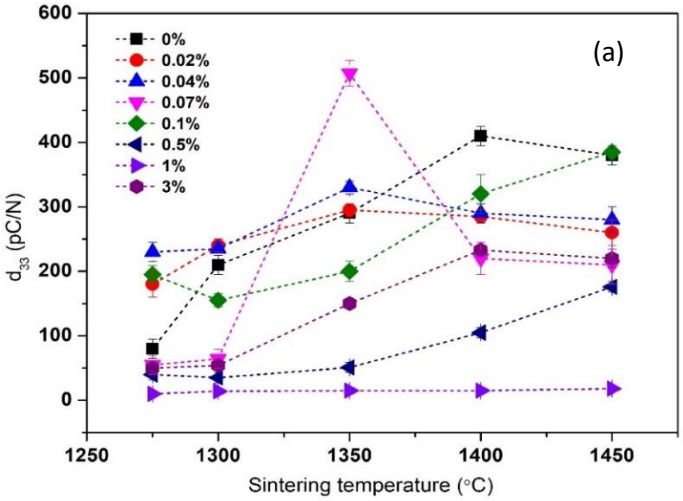

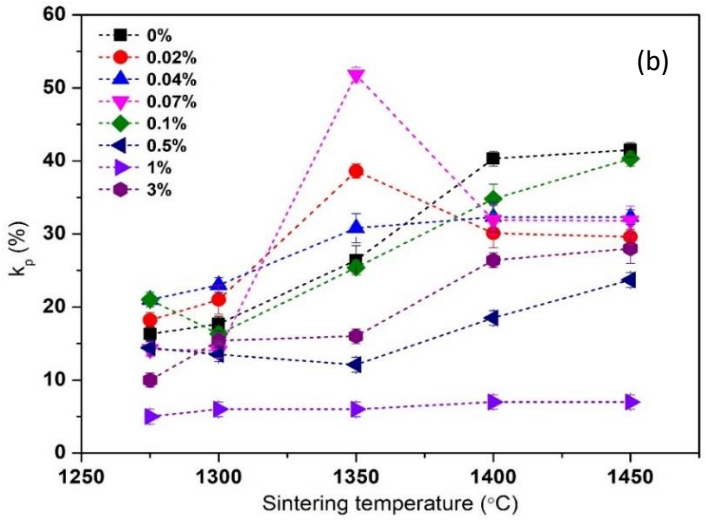

Fig. 6 The dependence of (a) piezoelectric coefficient, d_{33} and (b) Planar coupling factor, k_p on sintering temperature for BCZT-yCeO_2 samples.

As high piezoelectric, dielectric properties and high densification (see table 2) is observed at 1350°C/4h for the y = 0.07% composition, from hereon we show and discuss other properties including temperature dependent dielectric properties, crystal structural analysis and ferroelectric properties for samples sintered at this temperature only.

Table 2. Physical and functional properties of BCZT- $_y$$CeO_2$ ceramics sintered at 1350ºC/4h and measured at room temperature.

BCZT - $_y$$CeO_2$	*Bulk density (g/cm^3)*	*Grain Size (μm)*	*d_{33} (pC/N)*	*k_p (%)*	ε_r	*T_C (°C)*
y=0	4.93±0.05	7.6±2	290±15	26.4	1637±101	101.8
y=0.02	5.18±0.05	10.37±2	295±5	38.6	2650±150	101.4
y=0.04	5.57±0.05	9.9±2	330±10	30.8	3854±175	101.8
y=0.07	**5.64±0.04**	**13.56±2**	**507±20**	**51.8**	**4091±100**	**104.4**
y=0.1	5.43±0.04	6.43±3	200±16	25.4	2166±126	103.1
y=0.5	5.22±0.05	1.14±1	51±2	12.1	2651±150	97.5
y=1	4.66±0.03	1.61±0	-	-	1123±75	34.1
y=3	5.29±0.05	2.79±2	150±5	16	2692±200	106.2

4.3 Properties of BCZT-CeO_2 ceramics sintered at 1350°C for 4h

4.3.1 Temperature dependent dielectric properties.

The temperature dependence of the relative permittivity of BCZT-yCeO_2 ceramics sintered at 1350ºC/4h and measured at 1 kHz is shown in figure 7. Three peaks were observed for compositions in the range y = 0 - 0.1% that could be ascribed to the rhombohedral-orthorhombic (R-O), orthorhombic-tetragonal (O-T) and tetragonal-cubic (T-C) phase transitions [22]. The peak at ~ 0 - 5°C could not always be observed clearly from the relative permittivity data, therefore, in figure 8, the temperature dependence of the loss tangent for each composition are also shown. The three

phase transitions can be confirmed by the presence of three distinct peaks for compositions y = 0 - 0.1% with the rhombohedral-orthorhombic (R - O) phase transition at ~ 0 - 5°C, the O - T phase transition ~ 36 - 41°C and the T - C phase transition at ~ (100 - 104°C).

As the Ce concentration is increased from y = 0% to y = 0.07% the dielectric peaks appear sharper and the value of maximum relative permittivity (at the Curie Temperature) is increased from 7000 to nearly 14000. This also corresponds with an increase in grain size for this sintering temperature. For higher Ce concentrations (y > 0.1%) the maximum relative permittivity is drastically reduced (~ 4000) which may be due to the smaller grain size of these samples. Fine grains have also been reported to generally shift T_C towards lower temperatures due to internal stress in the materials which can be relieved by twinning mechanisms in larger grained samples [23, 24].

As the CeO_2 content is further increased from y = 0.5 - 1% the T_C decreased gradually to an indicative value of ~ 34°C. However, as discussed above, this composition does have anomalous behaviour in a number of measured properties. Furthermore, the general decrement of T_C may be related to the fine-grained specimens as previously reported with BCZT-Bi_2O_3 ceramics and in agreement with the stress model [25] or to the cell volume effect evolved by grain sizes [26] and will form the basis of future studies. It can also be seen that the dielectric peaks for samples with composition y = 0.5, 1 and 3% become diffuse around T_C (see figure 7), in line with their smaller grain size. The dielectric peak in small grain sized specimens is correlated to diffuse phase transition (DPT) that can be increased by minimizing the grain size [20,23]. The DPT occurs due to an existence of small micro regions in the ceramic, switching statistically from paraelectric to ferroelectric state but does not have interactions with neighbouring regions what so ever [23]. Which might indicate each region have an independent transition temperature.

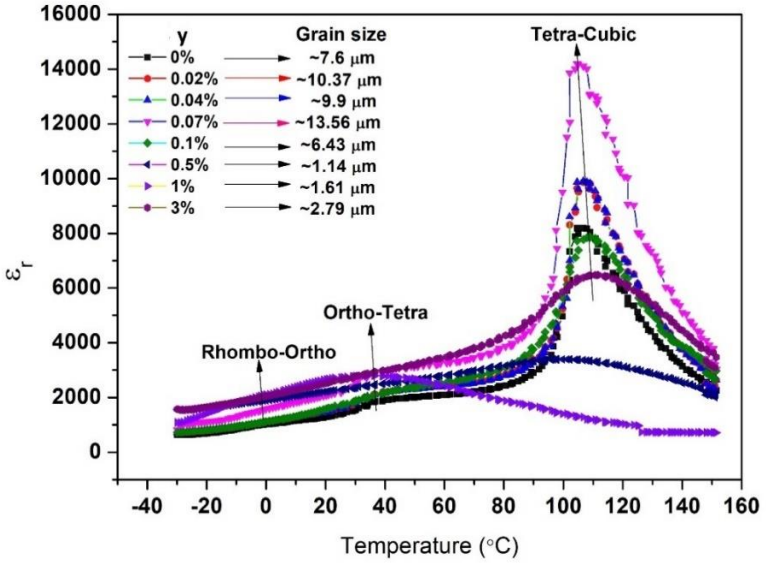

Fig. 7 Temperature dependence of relative permittivity of CeO_2-doped BCZT ceramics sintered at 1350°C/4h.

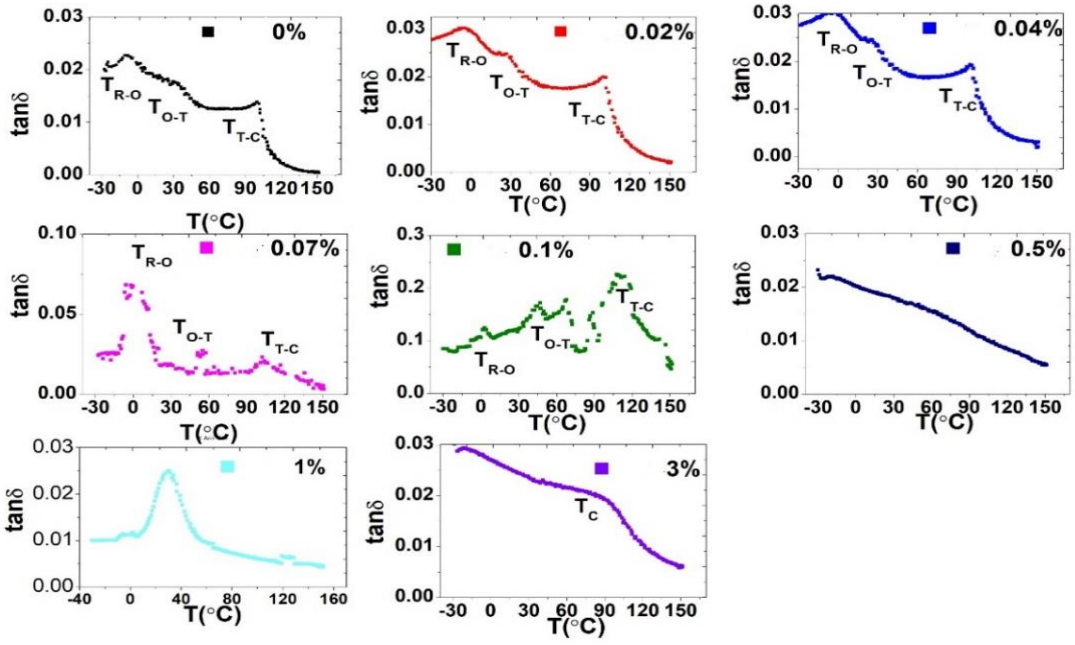

Fig. 8 Loss tangent of BCZT-yCeO_2 ceramics sintered at 1350°C/4h and measured at room temperature.

The plot between log $(1/\varepsilon_r - 1/\varepsilon_{r(max)})$ versus. log $(T - T_{max})$ of BCZT-yCeO_2 ceramics sintered at 1350°C/4h is depicted in figure 9. A modified Curie Weiss law proposed by Uchino and Nomura [27], to describe the diffuseness of ferroelectric phase transition is expressed as:

$$1/\varepsilon_r - 1/\varepsilon_{r(max)} = (T - T_{max})^{\gamma} / C$$

Where, T_{max} is a temperature at which dielectric constant (ε_r) is maximum, γ is diffusivity coefficient and C is Curie Weiss constant. The limiting value of γ=1 and γ=2 follow the Curie Weiss equation for normal ferroelectric and ideal relaxor ferroelectric transition respectively. A linear relationship is obtained from the logarithmic plots shown in figure 24 for all samples. Finally, the slope of the fitting curves was used to determine the γ values which is shown in the inset of figure 9. it can be noted that as the Ce content is increased, γ value also increased and reaches up to 1.9634 indicating an occurrence of a relaxor ferroelectric behaviour and is partially caused by domain refinement and higher inner stress due to the small grain size [20]. With increasing grain size, γ value was reduced gradually from 1.9634 to 1.6442. The values of C, T_o and γ with grain size is summarized in table 3.

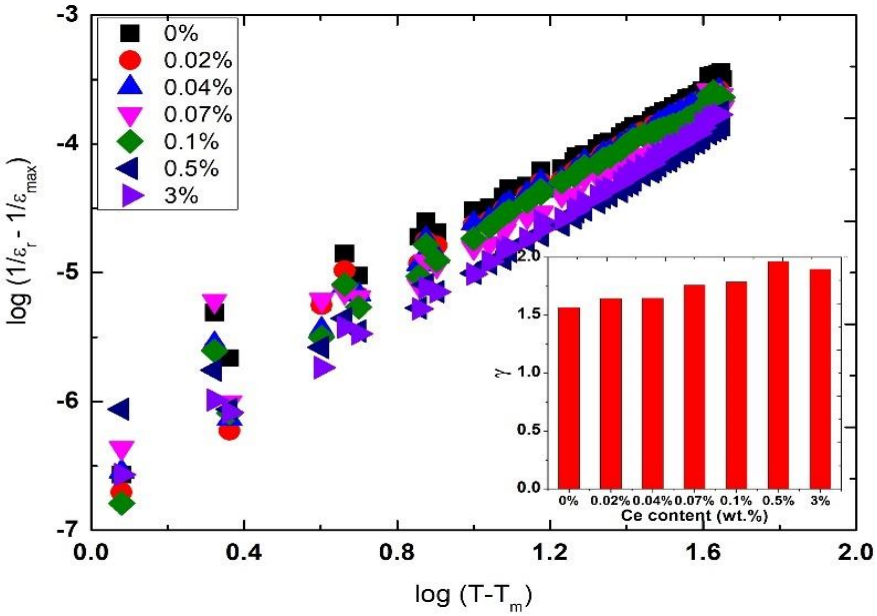

Figure 9. Plot between log ($1/\varepsilon_r - 1/\varepsilon_{r\,(max)}$) vs. log ($T - T_{max}$) of BCZT-y$CeO_2$ ceramics sintered at 1350°C/4h.

Table 3. The Curie–Weiss Temperature (To), the Curie–Weiss Constant (C) and the Diffuseness Coefficient (γ) for BCZT Ceramics at 1 kHz

Ce Content (y wt.%)	0%	0.02%	0.04%	0.07%	0.10%	0.50%	3%
Grain size (μm)	7.6±2	10.37±2	9.9±2	13.56±2	6.43±3	1.14±1	2.79±2
T_o [K]	373	374	375	380	364	320	358
C [10^5 K]	1.11	1.26	1.25	1.48	1.73	2.21	2.25
γ	1.5678	1.6445	1.6472	1.7595	1.7877	1.9634	1.8957

4.3.2 Crystal structure

4.2.2a X ray diffraction analysis

X ray diffraction analyses carried out at room temperature of BCZT- yCeO_2 ceramics sintered at 1350°C/4h are shown in figure 10(a). A pure perovskite phase is observed with no trace of secondary phase suggesting the Ce ions may diffuse into the BCZT solid solution, although any secondary phase may be below the detection limit. To analyze the influence of cerium on BCZT ceramics further analyses of the data have been carried out in the range of 2θ, 44°-47° and 82°- 85° as shown in figure 10(b) and figure 10(c) respectively. The splitting of the (200) peak into (002)/(200) at around 45° along with the splitting of the (222) peak into (222)/(-222) peaks at around 83° suggests a mixture of tetragonal and rhombohedral phases for the samples with compositions y=0 - 0.1%. Single (200) and (222) peaks for samples with composition y=0.5 & 1% indicate a pseudo cubic and cubic phase respectively. We are naming pseudo cubic phase since sample y=0.5% still show some d_{33} (table 4) which is discussed further below in Raman analysis (section 4.2.2b). While a single

(200) peak and split (222) reflections indicate a single phase rhombohedral symmetry for the y=3% composition. This analysis is consistent with previous reports [28 - 30].

The occupancy of the two cation sites in the perovskite structure is often analyzed in terms of tolerance factors, with smaller ions [$r(R^{3+})$] < 0.087 nm occupying the B site and larger ions [$r(R^{4+})$] > 0.094 nm occupying the A site. It is possible for ions with intermediate sizes to occupy either or both sites [31, 32]. Since Ce exists in both valance states as Ce^{3+} (ionic radii, 0.134 nm) and Ce^{4+} (0.087 nm) [33] therefore it is believed that Ce^{3+} ions may occupy A site of either Ca^{2+} (0.134 nm) or Ba^{2+} (0.161 nm) and Ce^{4+} ions occupy B site of either Ti^{4+} (0.060 nm) and Zr^{4+} (0.072 nm). It is well known in the case of another perovskite $BaTiO_3$, Ce^{3+} substitutes A site while Ce^{4+} substitute B site however self-compensation occurs when Ba/Ca = 1 [34]. Ce ions incorporated to the BCZT lattice might also cause disarrangement in the distribution of different ions at different sites leading to distortions and structural fluctuations that may result in the inferior properties. Table 4 represents the lattice parameters and phase structure of samples y=0 – 0.1%. samples y > 0.1% were identified either cubic or rhombohedral structures so are not included. It can be seen that the c/a ratio was in the range of 1.0035 - 1.0042 with coexistence of rhombohedral and tetragonal phase reflections indicating an existence of an MPB. As part of a study of undoped BCZT ceramics we have previously reported a tetragonal phase with c/a ratio ~ 1.0043 adjacent to an orthorhombic phase region [18] indicating nearly similar value for the sample y = 0.07% as depicted in table 4. The data presented here are thus consistent with the formation of a bridging orthorhombic phase between the rhombohedral and tetragonal phase regions, although the orthorhombic phase was not separately identified, and could be a basis for the existence of the MPB previously published [35].

Table 4. Cell parameters and c/a ratio for BCZT-yCeO_2 ceramics sintered at 1350°C/4h.

Sample BCZT-yCeO_2 (x in wt.%)	a (Å)	b (Å)	c (Å)	Phase structure	Average c/a ratio
y=0	3.998	3.998	4.012	Rhombohedral-Tetragonal	1.0035
y=0.02	3.998	3.998	4.013	Rhombohedral-Tetragonal	1.0037
y=0.04	3.998	3.998	4.014	Rhombohedral-Tetragonal	1.0040
y=0.07	3.998	3.998	4.015	Rhombohedral-Tetragonal	1.0042
y=0.1	3.999	3.999	4.014	Rhombohedral-Tetragonal	1.0037

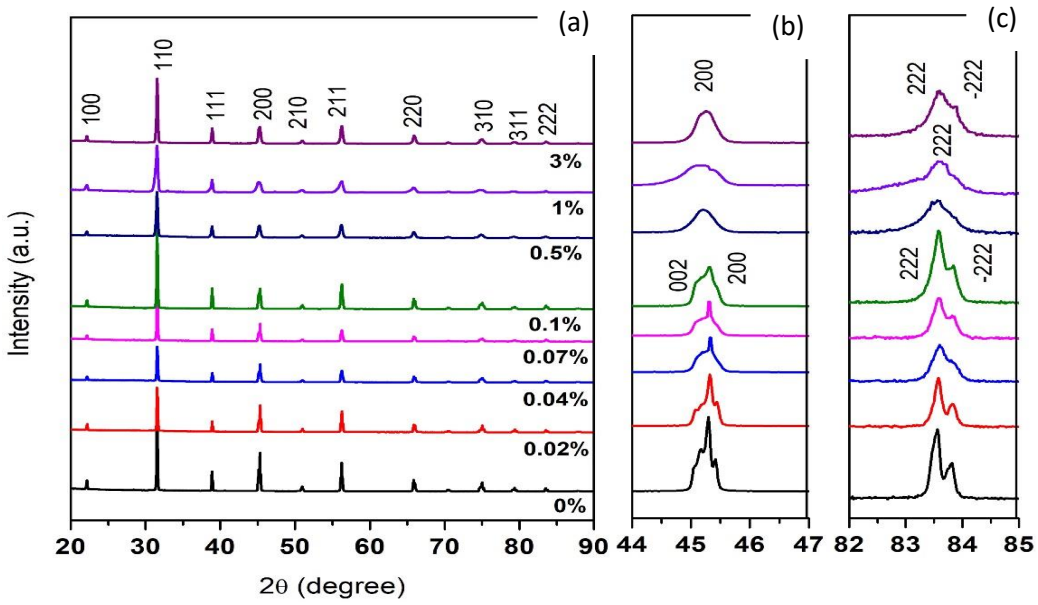

Fig.10. XRD patterns of BCZT-yCeO_2 ceramics sintered at 1350°C/4h

4.2.2b Raman spectra

Figure 11 shows evolution of Raman spectra of BCZT-yCeO_2 ceramics with different Ce concentration at 1350 °C/4h. Modes at 93, 153,196, 249, 293, 524, 730 cm^{-1} observed at room temperature for samples 0 ≤ y ≥ 0.1 wt.%. These modes are related to both R phase especially at about 153 and 196 cm^{-1} and T phases (including modes 249, 293, 524, 730 cm^{-1}) which agrees with previous reports [36 – 39]. Previous reports suggest that for mode at 490 cm^{-1} is important to confirm the O phase but here for the samples y=0 - 0.1% we could not have observed the 490 cm^{-1} mode [38] which can be seen by single sharp peak at 524 cm^{-1}. It suggests that 490 cm^{-1} peak merges with 524 cm^{-1} peaks. Therefore, it is believed that R and T phases coexisted for the samples y=0 - 0.1% at room temperature. Meanwhile the intensity of the peaks gets weak and modes 153, 196, cm^{-1} disappeared which indicates disappearance of R phase for the samples y = 0.5 and 1 %. In addition, disappearance of mode 293 cm^{-1} and low intensity peaks at around 293, 524 and 730 cm^{-1} indicate that T phase has also reduced but not vanishes completely. Also, broad modes of 249 and 524 cm^{-1} are the feature of C phases [40] for y = 0.5 and 1%. Hence it is speculated that pseudo cubic phase might exist for the samples y= 0.5 and 1 %. For 3% sample, although the intensity of the modes 153, 193 cm^{-1} are very low but still can be seen and disappearance of 249 cm^{-1} and 490 cm^{-1} indicates single weak R phase as shown in the figure 11. These results are in close agreement with the XRD analysis discussed in section 3.4.1a.

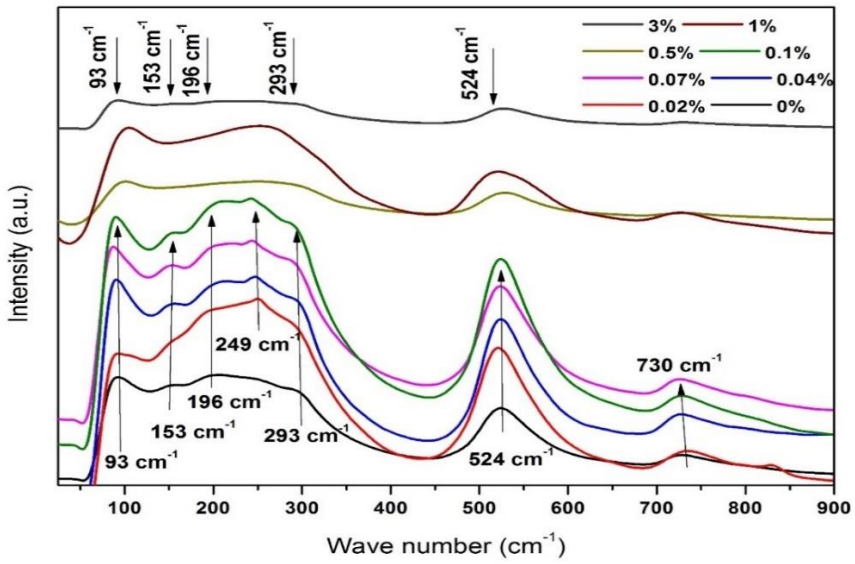

Figure 11. Raman spectra of BCZT-yCeO_2 ceramics sintered at 1350°C/4h and measured at room temperature

(II) BCZT-yCeO_2 ceramics sintered via two step sintering technique (TSS)

In this follow up, the green bodies of BCZT - $_yCeO_2$ (y = 0, 0.02, 0.04, 0.07 wt.%) were processed at same conditions stated in section 5.1. As discussed earlier in section 6.5.2a, that the MPB was found in the $_yCeO_2$ composition range (y = 0 – 0.1 %) and high functional properties were observed in this range (table 2). Based on these findings via conventional sintering technique, CeO_2 content range (y = 0, 0.02, 0.04, 0.07 wt.%) were chosen. Then pressed green bodies were sintered via TSS technique shown in figure 1(b). In the first step the furnace was programmed at rapid ramp up rate 10 °C/min to a temperature T_1 (1350, 1400, 1450 °C) with 30 min dwell just to ensure the uniformity of heat atmosphere inside the chamber. Then the furnace was cooled rapidly 30 °C/min to the lower temperature T_2. This temperature is fixed at 1275 °C to lock the grain growth and kept here for 4 hours. Finally, the temperature is ramped down to the room temperature at the rate 10 °C/min.

4.4 Bulk density, microstructures and grain size

Bulk densities were calculated for BCZT-yCeO_2 ceramics as depicted in figure 12. For each composition, the ceramics were sintered at different sintering conditions and their density were calculated. As Ce concentration increases Bulk densities increases and achieved maximum 5.73 g/cm^3 for y = 0.07 wt.% at sintering condition, T_1 - 1400 °C/30min and T_2 - 1275 °C/4h which is almost 99% of the theoretical density for BCZT ceramics (5.81 g/cm^3) previously reported [16]. Here for y = 0 wt.% bulk density is calculated as 4.78 g/cm^3 (~ 82% of t.d.) at sintering condition, T_1 - 1400 °C/30min which clearly suggests that Ce ions are effective while promoting densification of BCZT ceramics.

The microstructure of these ceramics has been observed by SEM for samples sintered at sintering condition, T_1 - 1350 °C/30min and T_2 – 1275 °C/4h and is shown in figure 13. Pure BCZT (y = 0 wt.%) has an obvious porous microstructure at this sintering temperature. As the Ce content increased to 0.04 wt.% it seems that there was no improvement in densification but when y = 0.07 wt.% the microstructure becomes fully dense. The microstructure (y = 0.07 wt.%) has non-uniform grains which might affect the properties of these ceramics. At sintering condition, T_1 – 1400 °C/30min and T_2 – 1275 °C/4h it is evident that CeO_2 incorporation causes densification and uniform microstructure (y = 0.07%) as depicted in figure 14. Samples y = 0 - 0.04 wt.% remain still porous. As the sintering temperature further increased to T_1 – 1450 °C/30min the samples y = 0 - 0.04 % densify a little but sample y= 0.07 % started to become porous as can be seen in the figure 15. This supports the bulk density data depicted in figure 12.

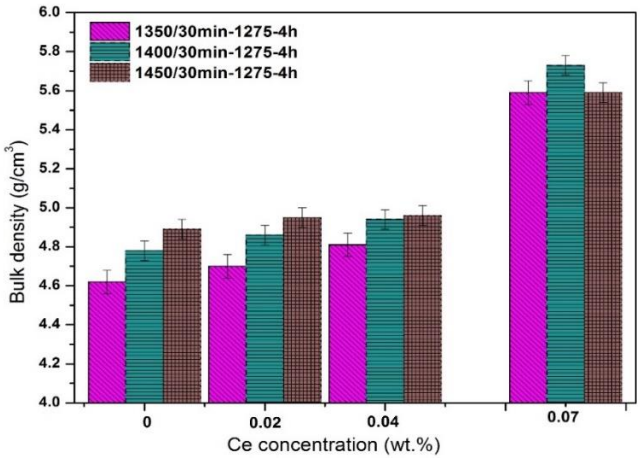

Fig. 12 Bulk densities as a function of Ce content at different sintering temperature via TSS.

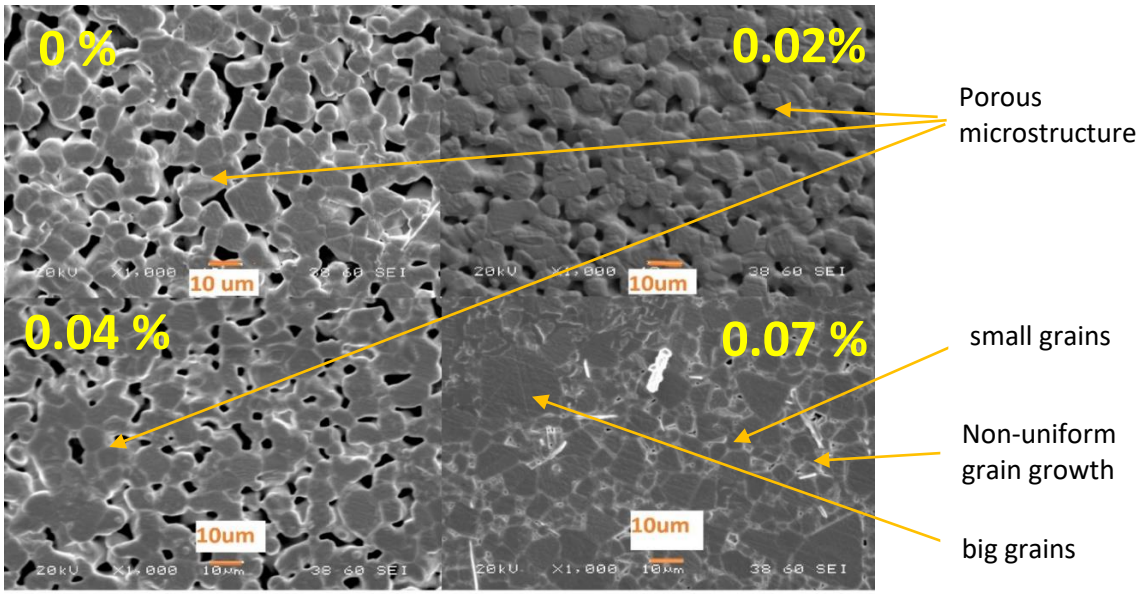

Fig. 13 SEM microstructure of BCZT-yCeO_2 ceramics (a) y = 0% (b) y = 0.02% (c) y = 0.04% (d) y = 0.07% at T_1 – 1350 °C/30 min &T_2 – 1275 °C/4h

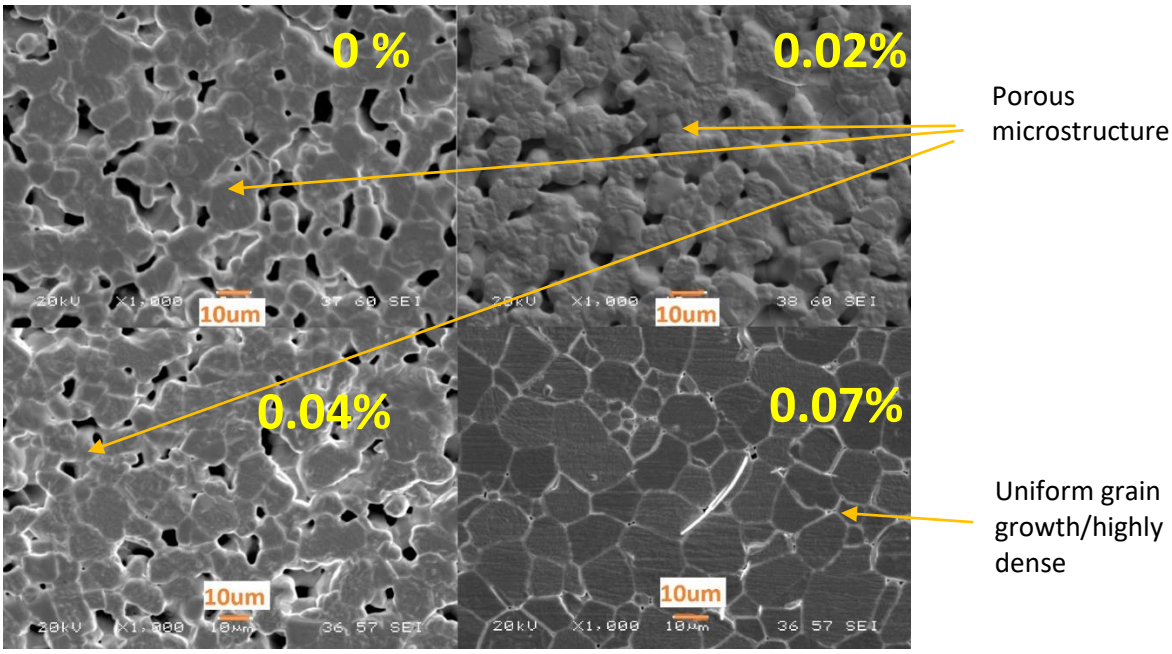

Fig. 14 SEM microstructure of BCZT-yCeO₂ ceramics (a) y = 0% (b) y = 0.02% (c) y = 0.04% (d) y = 0.07% at T_1 – 1400 °C/30 min & T_2 – 1275 °C/4h

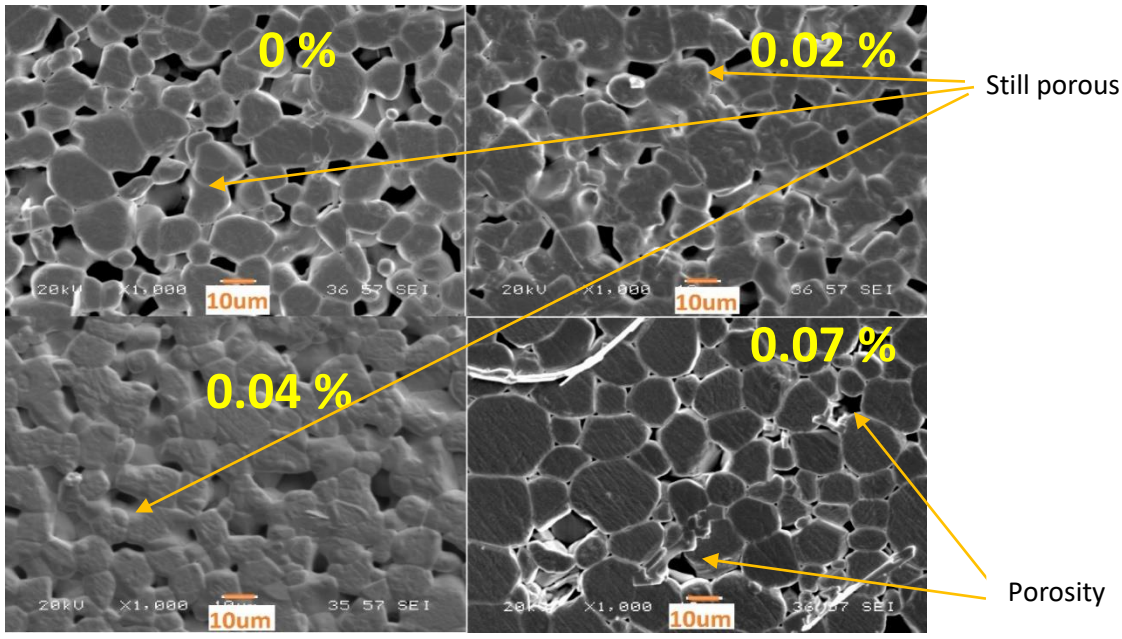

Fig. 15 SEM microstructure of BCZT-yCeO₂ ceramics (a) y = 0% (b) y = 0.02% (c) y = 0.04% (d) y = 0.07% at T_1 – 1450 °C/30 min & T_2 – 1275 °C/4h

The average size of the grains was calculated to be < 10 μm for all samples at different sintering temperatures as shown in figure 16 which clearly indicates that the TSS technique can play an

important role in reducing grain size while maintaining highly dense microstructures compared to conventional sintering.

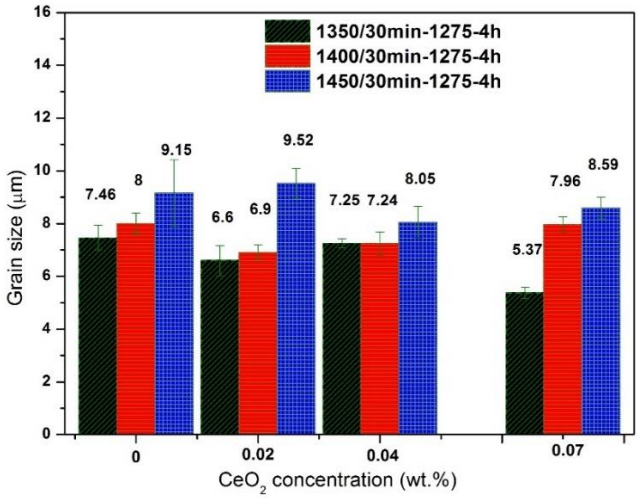

Fig. 16 Grain size of BCZT-yCeO_2 (y = 0 - 0.07 wt.%) ceramics at different sintering conditions via TSS.

Therefore, we consider optimum sintering conditions as the temperature at which the density is maximum. Here in this case sintering conditions, T_1 – 1400 °C/30min and T_2 – 1275 °C/4h is the optimum sintering conditions, therefore, we are showing piezoelectric, dielectric and ferroelectric properties of samples sintered at these sintering conditions in Table 5 and 6.

4.5 Functional properties

Table 5 and Table 6 shows functional properties of BCZT-yCeO_2 ceramics at sintering condition, T_1 – 1400 °C/30min & T_2 – 1275 °C/4h. Clearly sample y – 0.07 wt.% shows excellent properties compare to other samples. From TSS, the piezoelectric properties reduced a little as compare to the conventional sintering. This reduction may be ascribed to the small grain sizes (< 10um).

Table 5. Piezoelectric and dielectric properties of BCZT-yCeO_2 ceramics at sintering condition, T_1 – 1400 °C/30min & T_2 – 1275 °C/4h.

BCZT - $_yCeO_2$	*Grain Size (μm)*	*d_{33} (pC/N)*	*k_p(%)*	*ε_r*	*T_C (°C)*
y=0	8.0±0.75	295±15	23.2±2	1906±80	103.4
y=0.02	6.9±0.29	315±10	28.1±1	2193±80	100.1
y=0.04	7.24±0.44	340±10	28.9±2	2308±80	101.2
y=0.07	**7.96±0.71**	**353±7**	**40±1**	**3393±100**	**96.2**

Table. 6. Ferroelectric properties of BCZT-yCeO_2 ceramics at sintering conditions, T_1 – 1400 °C/30min and T_2 – 1275 °C/4h

BCZT-yCeO_2	*P_r ($\mu C/cm^2$)*	*P_{max} ($\mu C/cm^2$)*	*S_{max} (%)*	*E_C (kV/cm)*
y = 0%	4.22	10.52	0.11	3.17
y = 0.02%	5.00	12.00	0.13	2.45
y = 0.04%	5.65	13.00	0.14	2.47
y = 0.07%	**11.61**	**20.26**	**0.18**	**2.32**

(III)A-site substitution of CeO_2: Synthesis and characterization of $(Ba_{0.85}\ Ca_{0.15-y}\ Ce_y)\ (Zr_{0.1}\ Ti_{0.9})\ O_3$ ceramics

4.6 Bulk density, microstructures and grain sizes

It is expected that as the sintering temperature goes up the bulk density also increases as depicted in figure 17. Density higher than 5.40 g/cm³ is observed for samples y> 0 sintered at temperature 1350 °C. Maximum density of 5.75 g/cm³ was achieved for x = 0.02. Figure 18 and figure 19 shows microstructures of these ceramics sintered at 1350 °C and 1450 °C respectively. For samples sintered at 1350 °C the microstructures of y= 0, 0.0008 and 0.00135 are not dense enough as compared to the sample y = 0.02. For samples sintered at 1450 °C, grains grow rapidly which increased densities of the samples in the range y = 0 - 0.00135.

It is evident that CeO_2 addition causes a significant change in the grain sizes. Pure BCZT (y = 0) ceramics have a porous microstructure with small grains at 1350°/4h as shown in figure 18. However, when a small amount of CeO_2 is introduced, a comparatively dense microstructure with enlarged grains is developed (figure 18b, 18c). A similar trend has been found at the higher sintering temperature 1450°C/4h (figure 19b, 19c). It seems that CeO_2 addition at amount less than or equal to 0.00135 enhances the grain growth. However, CeO_2 addition larger than 0.00135, the grain sizes do not change significantly with the sintering temperature. Hence, the amount of CeO_2 in BCZT composition concerns a change in the grain size. However, sample y=0.02 shows very limited grain growth, irrespective of increasing sintering temperature, which might indicate that the higher amount of CeO_2 is effective in suppressing the grain growth of BCZT ceramics during sintering. Similar results have been found previously with different compositions [19, 41].

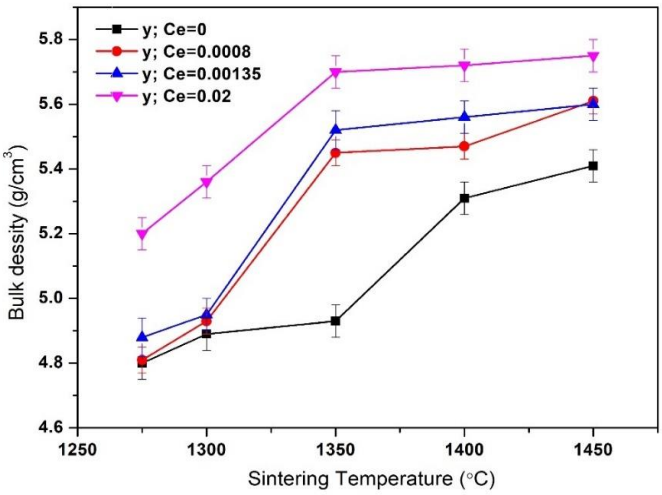

Fig. 17 Bulk density as a function of sintering temperature of $(Ba_{0.85}\,Ca_{0.15-y}\,Ce_y)\,(Zr_{0.1}\,Ti_{0.9})\,O_3$ ceramics

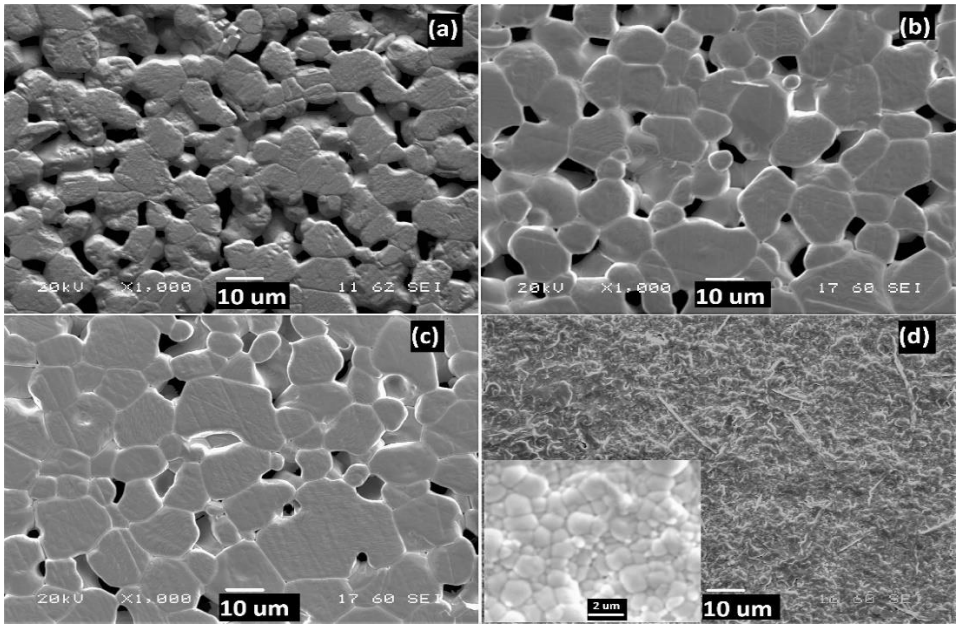

Fig. 18 SEM images of $(Ba_{0.85}\,Ca_{0.15-y}\,Ce_y)\,(Zr_{0.1}\,Ti_{0.9})\,O_3$ ceramics for x values of (a) 0 (b) 0.0008 (c) 0.00135 (d) 0.02 sintered at 1350 °C for 4 h.

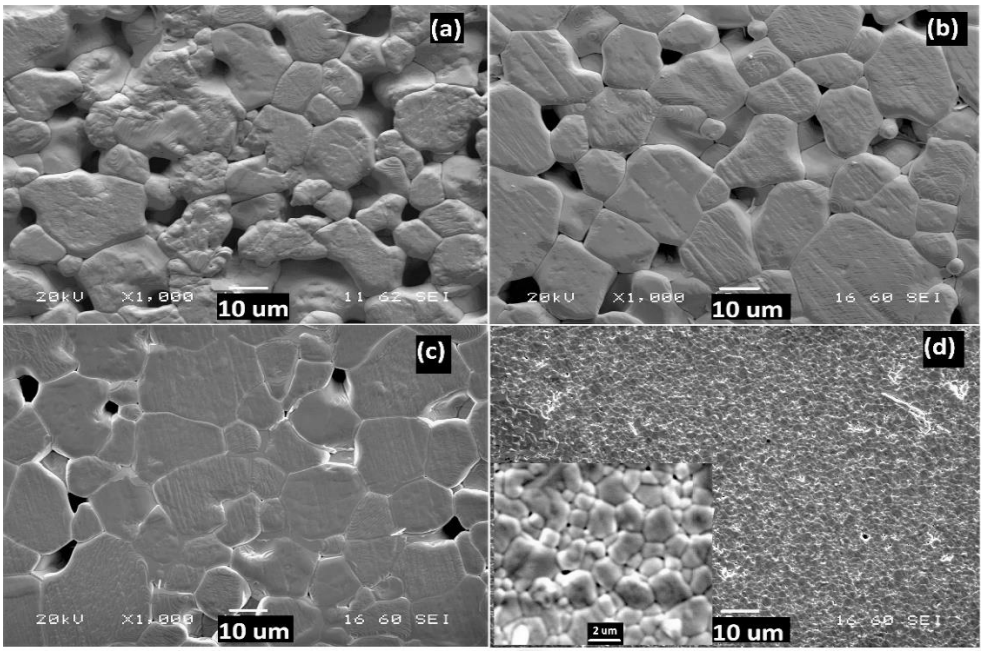

Fig. 19 SEM images of $(Ba_{0.85}Ca_{0.15-y}Ce_y)(Zr_{0.1}Ti_{0.9})O_3$ ceramics for x-values of (a) 0 (b) 0.0008 (c) 0.00135 (d) 0.02 sintered at 1450 °C for 4 h.

4.7 Functional properties

Figure 20 and figure 21 show piezoelectric coefficient (d_{33}) and planar coupling factor (k_p) respectively with different sintering temperatures. As the sintering temperature increases d_{33} values increases and achieved maximum for y= 0.00135 sintered at 1350 °C and then decreases drastically with higher temperatures. For samples sintered at 1350°C, pure BCZT (y = 0) has d_{33} value ~ 290 pC/N with relatively low grain size ~ 7.6 µm. As the Ce concentration is slightly increased, grains grow (> 11 µm) and subsequently d_{33} value has increased and observed maximum as 501±10 pC/N for sample y = 0.00135. On further increase in Ce concentration to 0.02, d_{33} reduces which may attributed to very fine grain size ≃ 0.76 µm. Planar coupling factor follows the same trend with the grain size and was observed maximum value = 38.5% for y = 0.00135 sintered at 1350 °C/4h plotted in figure 21.

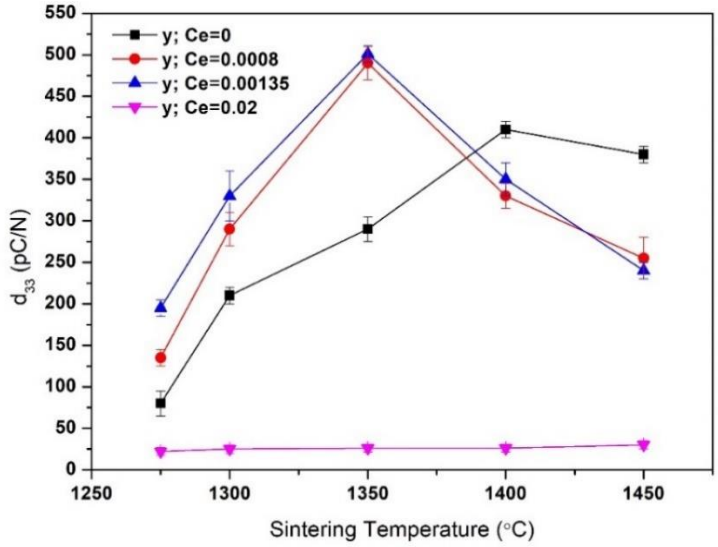

Fig. 20 Piezoelectric constant against sintering temperature of $(Ba_{0.85}Ca_{0.15-y}Ce_y)(Zr_{0.1}Ti_{0.9})O_3$ ceramics

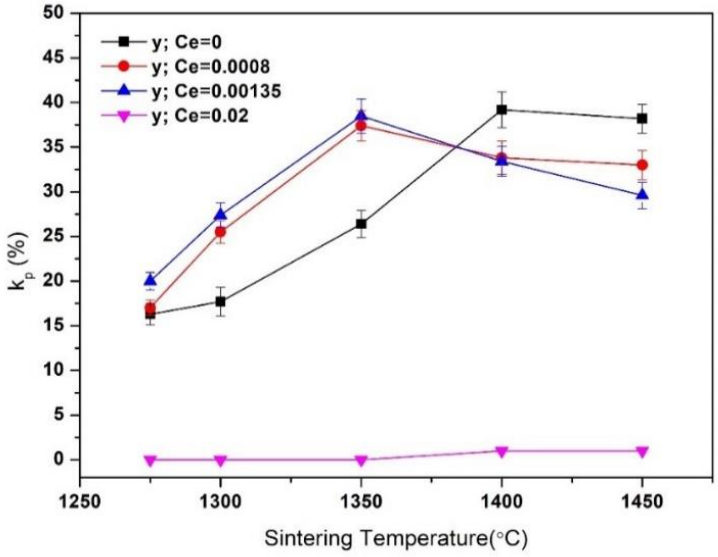

Fig. 21 Planer coupling coefficient against sintering temperature of $(Ba_{0.85}Ca_{0.15-y}Ce_y)(Zr_{0.1}Ti_{0.9})O_3$ ceramics

Table. 7 Summary of piezoelectric properties and Curie temperature with grain size of $(Ba_{0.85}Ca_{0.15-y}Ce_y)(Zr_{0.1}Ti_{0.9})O_3$ ceramics sintered at 1350°C/4h.

y=mol.	Grain size(μm)	d_{33} (pC/N)	k_p (%)	T_C (°C)
0	7.6±2	290±15	26.4±1	105.4
0.0008	12.16±2.39	490±20	37.8±1.69	103.2
0.00135	11.26±1.97	501±10	38.5±1.92	108.1
0.02	0.76±0.08	60±05	8.5±1.35	72.6

P-E hysteresis loops for $(Ba_{0.85}Ca_{0.15-x}Ce_x)(Zr_{0.1}Ti_{0.9})O_3$ are shown in figure 22(a) for samples sintered at 1350 °C/4h. All samples exhibit typical ferroelectric loops under switching frequency 1 Hz. Here again we observed that the remenant polarization (P_r) significantly depends on the grain sizes. For pure BCZT (x = 0) the P_r is around 7.86 (μC/cm²) (7.6±2 μm, grain size) and when cerium content is increased up to 0.00131, P_r has increased 12.19 (μC/cm²) (11.26±1.97 μm, grain size). On further increment in cerium as y = 0.02, grain size reduced (0.76 μm) drastically, decreasing P_r to 3.68(μC/cm²). In addition, the coercive field is quite large (> 5 kV/cm) for all the samples which is mainly due to porous microstructure for the samples (y = 0 - 0.00135). However, coercive field was reduced slightly (3.14 kV/cm) for the sample y = 0.02 due to the improved density but still quite large compare to BCZT-yCeO2 ceramics ~ 2 kV/cm. Very small grain size may be another reason for large coercive field.

A study on P-E response due the grain size of the ceramics has been proposed by Ohihara [42] in which fractions (f) of grains give rise to the polarization reversal or domain switching and it is expressed as:

$$f = f_o(1 - \exp(-G_a d^3 / kT)) \qquad (22)$$

where f_o is the initial polarization or domain of ferroelectric materials, G_a is a constant that represents grain anisotropy energy density, d is grain size of the ceramics. Based on these conclusions '*f*' has only importance with the grain size d. Therefore, if the grain size increases, the fraction of grains contributing the reversal of polarizations also increases which can bring about the improvement in ferroelectric (P-E) nature. However, the space charge, or leakage may contribute to this P-E response, not only grain size effect, as can be seen by unsaturated polarization under high electric field (figure 22a).

Figure 23(b) represents strain- electric field (S-E) loops. A typical butterfly nature was observed for all the samples sintering temperature 1350 °C/4h. Pure BCZT (y = 0) with small grain size (7.6±2 μm) shows strain in the order of 0.11 % which is consistent with the density and P_r characteristics shown in figure 17 and figure 22a. As Ce concentration slightly increased up to 0.00131 mol. the grain size started to improve (> 11 μm) which results in better strain characteristics (~ 0.14%). Further increase in Ce concentration (0.02) resulted in smaller grain size (0.76±0.08 μm) and consequently

gives rise to the lower strain (0.07%) value. In such small grains, presence of non-180° domain walls are very difficult and preferably it is regarded as single grain or single domain having unrelieved/non-distressed internal stress. With increase in grain size, 90° domain wall presence can be more probable that can contribute more strain due to the easy movement of domain walls.

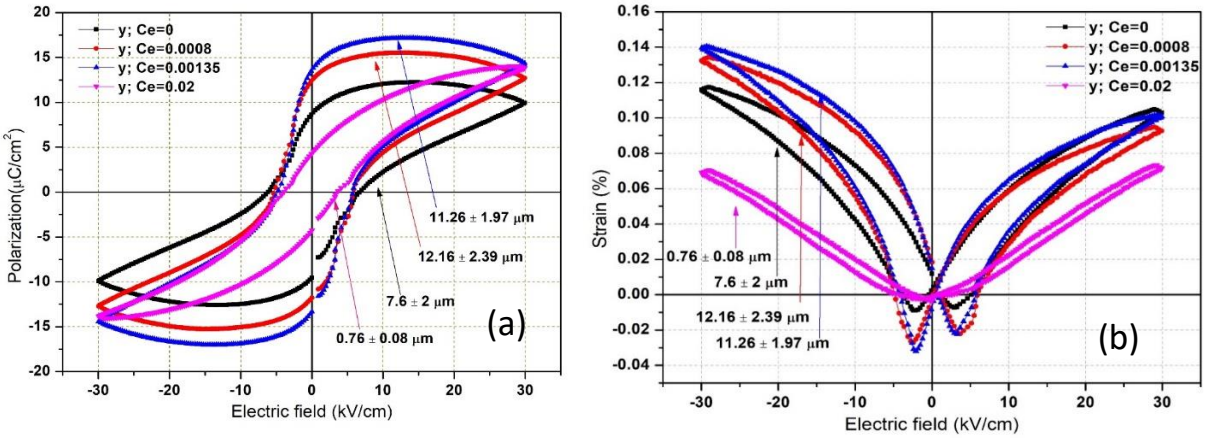

Fig. 22(a) Ferroelectric hysteresis loops and (b) Strain hysteresis loops for $(Ba_{0.85}Ca_{0.15-y}Ce_y)(Zr_{0.1}Ti_{0.9})O_3$ ceramics sintered at 1350 °C/4h

(IV) A-site substitution of CeO_2: Synthesis and characterization of $(Ba_{1-x-y}Ca_xCe_y)(Zr_{0.1}Ti_{0.9})O_3$ ceramics

$(Ba_{1-x-y}Ca_xCe_y)(Zr_{0.1}Ti_{0.9})O_3$ ceramics were prepared where x = 0.05, 0.10, 0.15, 0.20 mol. and y = 0.00135 mol. via conventional solid-state reaction method. The reason of choosing this composition is to see the effect of substitution of CeO_2 at A site of BCZT ceramics, where CeO_2 (y in the composition) is fixed as y = 0.00135 while barium and calcium molar ratios are changing. Also, it was found earlier in section 6 (I) and 6(II), small amount of CeO_2 incorporation could enhance the grain size which was one of the important reason to increase the piezoelectric properties. Since we have got the high piezoelectric properties when CeO_2 content was 0.00135 mol. (section 6 III) therefore, it is worth to investigate structural, microstructural and functional properties with this Ce content and varying A site elements (Ba & Ca) of $(Ba_{1-x-y}Ca_xCe_y)(Zr_{0.1}Ti_{0.9})O_3$ composition.

4.8 Bulk density, microstructures and grain size

Microstructures of $(Ba_{1-x-y}Ca_xCe_y)(Zr_{0.1}Ti_{0.9})O_3$ ceramics sintered at different temperatures are presented in figures 23, 24 and 25. Porous microstructures were observed for all samples at low sintering temperature, 1350°C/4h as shown in figure 23. When x;Ca content is low (0.05 and 0.10) there seems less porosity compared to the increased x;Ca content (0.15 and 0.20) at 1350°C/4h. The

grain grew, and the number of porous structure reduced when the sintering temperature was increased up to 1450 °C (figure 24,25). The grain size at 1350 °C is small (figure 23) for the samples x; Ca = 0.05 and 0.10 which could deteriorate its functional properties.

The measured bulk density of these ceramics is shown in figure 26. Densities of different compositions were increased with increasing sintering temperature (see figure 26). On the other hand, as the Ca content is increased from 0.05 to 0.20, reduction in densities were observed at every single sintering temperature. This could be due to the replacement of lighter Ca with heavier Ba. Because of the fact that ionic radius of Ca^{2+} is smaller that $Ba^{2+,}$ this could lead deformation in the system and mass transport for diffusion may be weakened. Fig. 27 shows grain size dependence on sintering temperatures and increases with increasing sintering temperatures.

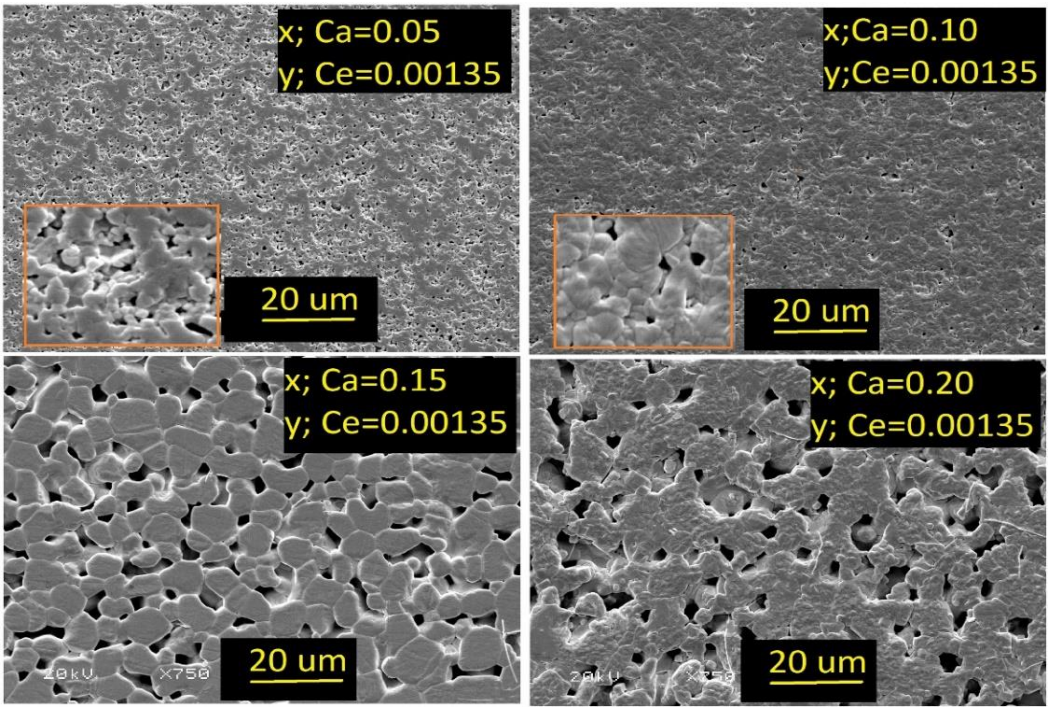

Fig. 23 Microstructure of $(Ba_{1-x-y}\ Ca_x\ Ce_y)\ (Zr_{0.1}\ Ti_{0.9})\ O_3$ ceramics at 1350 °C/4h

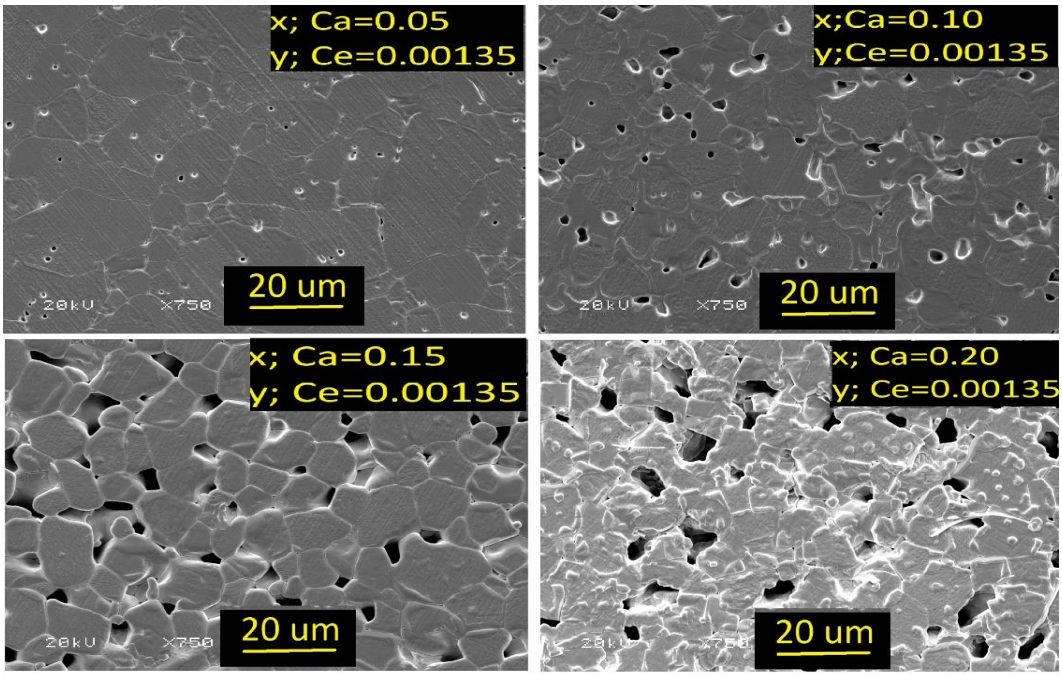

Fig. 24 Microstructure of $(Ba_{1-x-y}\ Ca_x\ Ce_y)\ (Zr_{0.1}\ Ti_{0.9})\ O_3$ ceramics at 1425 °C/4h

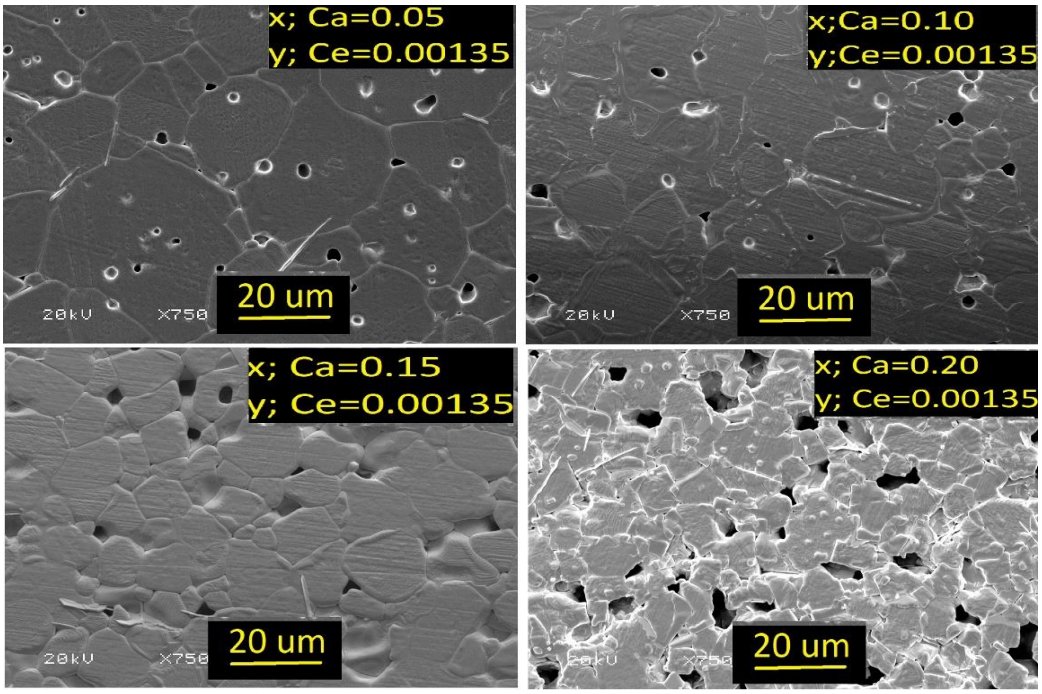

Fig. 25 Microstructure of $(Ba_{1-x-y}\ Ca_x\ Ce_y)\ (Zr_{0.1}\ Ti_{0.9})\ O_3$ ceramics sintered at 1450 °C/4h

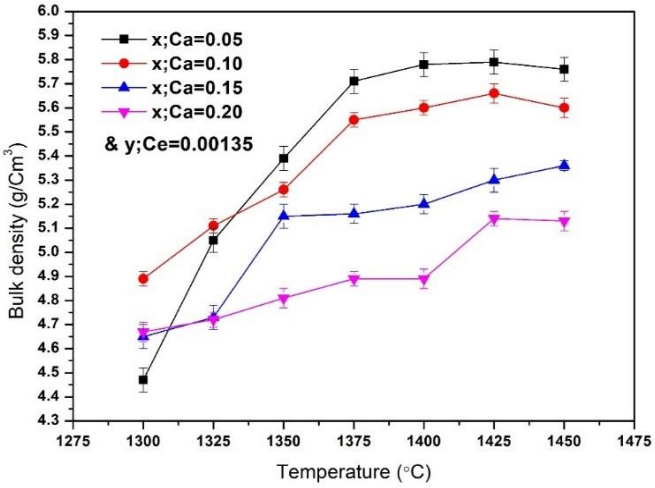

Fig. 26 Bulk densities of $(Ba_{1-x-y}\ Ca_x\ Ce_y)\ (Zr_{0.1}\ Ti_{0.9})\ O_3$ ceramics at different temperatures

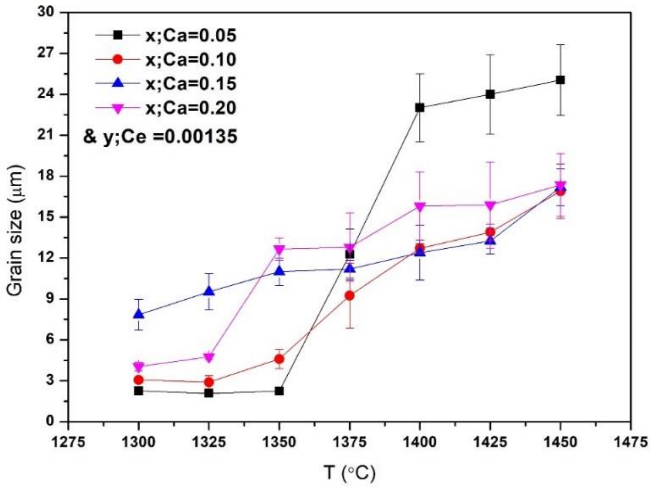

Fig. 27 Grain sizes of $(Ba_{1-x-y}\ Ca_x\ Ce_y)\ (Zr_{0.1}\ Ti_{0.9})\ O_3$ ceramics as a function of sintering temperature.

4.9 Functional properties

Piezoelectric properties including d_{33} and k_p are shown in figure 28 and figure 29 for different sintering temperatures from 1300 – 1450°C/4h, where x (Ca content) = 0.05, 0.10, 0.15, 0.20 and y (Ce content) is fixed as 0.00135. The corresponding Ba contents are 0.94, 0.89, 0.84 and 0.79. Since increase in sintering temperature may cause better grain growth and grain sizes as depicted in figure 27, which is an understandable cause of improvement in piezoelectric properties. For x;Ca = 0.05, 0.10, 0.20, relatively low piezoelectric properties obtained even at higher temperature (1450 °C/4h) as d_{33} = 205±10, 330±10, 290±20 pC/N and k_p = 30.2±2, 40±1, 32.2±1 % respectively where grain

size > 16 μm. The best properties were discovered when grain size ~ 13 um for x = 0.15 at relatively low temperature (1425 °C/4h) where d_{33} = 457±15 pC/N and k_p = 42.8 ± 1%.

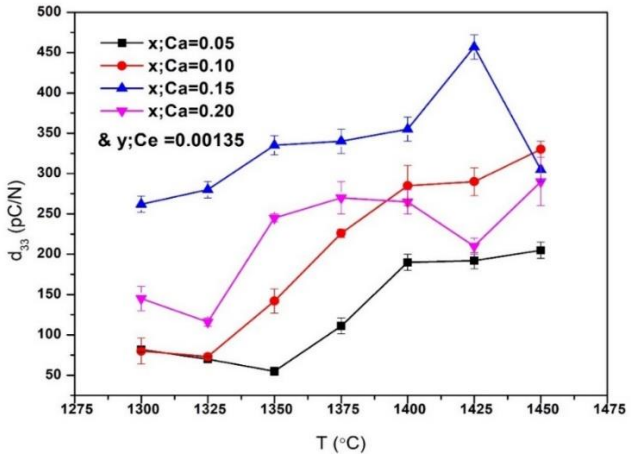

Fig. 28 Piezoelectric constants of $(Ba_{1-x-y}\ Ca_x\ Ce_y)\ (Zr_{0.1}\ Ti_{0.9})\ O_3$ as a function of sintering temperature.

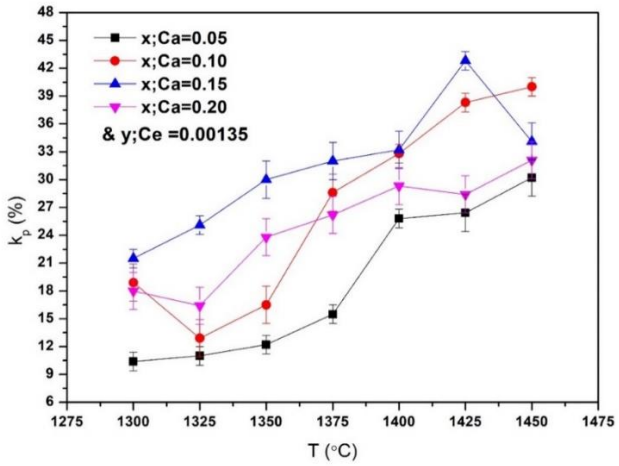

Fig. 29 Planer coupling coefficients of $(Ba_{1-x-y}\ Ca_x\ Ce_y)\ (Zr_{0.1}\ Ti_{0.9})\ O_3$ as a function of sintering temperature.

The temperature dependence of the dielectric constant is shown in figure 30 for samples sintered at 1425 °C/4h. Here in our choice of composition, $(Ba_{1-x-y}\ Ca_x\ Ce_y)\ (Zr_{0.1}\ Ti_{0.9})\ O_3$, Ca content 0.05, 0.10, 0.15 and 0.20 are very close to the 0.80BZT-0.20BCT, 0.66BZT-0.34BCT, 0.50BZT-0.50BCT, 0.30BZT-0.70BCT compositions respectively, previously shown according to (1-x)BZT - xBCT compositional phase diagram by Lui and Ren [12]. As can be seen from figure 30, two clear phase transitions can be observed above room temperature for the samples x; Ca = 0.05, 0.10, 0.15 corresponding to orthorhombic - tetragonal (O-T) and tetragonal - cubic (T-C) respectively. With further increase in Ca content (x;Ca =0.20), the orthorhombic-tetragonal phase could not be observed clearly. The T_{O-T} phase transition decreased obviously with increase in Ca content. Similar

results have been found by Liu and Ren [12] previously, where ε_{max} at T_C were reduced for large BCT composition in (1-x)BZT-xBCT phase diagram. It was observed that the phase transition T_{O-T} shifted towards room temperature below 30 °C with increasing Ca content and T_C is observed around 100 °C. Here, between x; Ca = 0.05 to 0.10, the relative permittivity is found in the range 13500 – 15000 which is nearly similar values reported previously [12]. While as Ca content increased (> 0.15) the dielectric or other properties will be deteriorated which is also observed here with reduced permittivity (~9000) at T_C. These results indicate that the Ca and Ba molar ratios may affect phase transition as well as dielectric properties. Phase transition peak shifting might also imply that certain Ce^{3+} ions entered the lattice of the perovskite structure. Table 8 represents functional properties which includes piezoelectric, dielectric and ferroelectric properties of these ceramics.

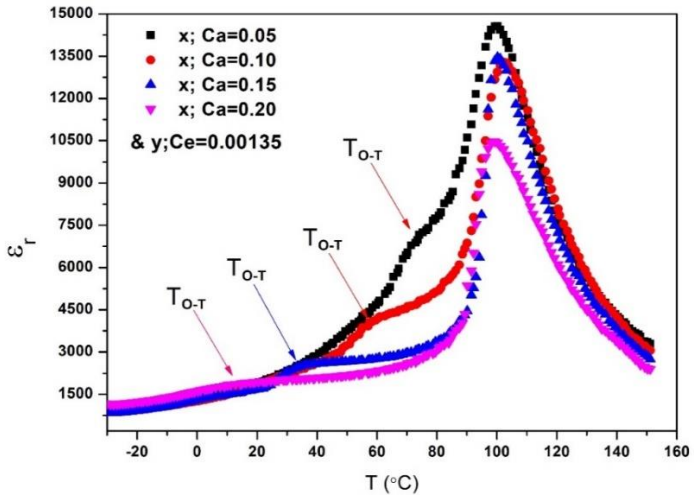

Fig. 30 Temperature dependent dielectric properties of $(Ba_{1-x-y}\ Ca_x\ Ce_y)\ (Zr_{0.1}\ Ti_{0.9})\ O_3$ ceramics sintered at 1425 °C/4h

Table 8. Summary of functional properties of $(Ba_{1-x-y}\ Ca_x\ Ce_y)\ (Zr_{0.1}\ Ti_{0.9})\ O_3$ ceramics sintered at 1425 °C/4h

Samples	Grain size (um)	d_{33} (pC/N)	k_p (%)	$\varepsilon_{r\ (max)}$	P_r ($\mu C/cm^2$)	E_C (kV/Cm)	S_{max} (%)
x=0.05 & y=0.00135	24±2.9	192±10	26.4±2	14562	7.49	3.28	0.11
x=0.10 & y=0.00135	13.89±0.6	290±15	38.3±1	13281	10.14	2.05	0.13
x=0.15 & y=0.00135	13.25±0.95	457±15	42.8±1	13461	10.85	2.02	0.14
x=0.020& y=0.00135	15.89±3.1	210±10	28.4±2	10466	5.02	4.13	0.12

4.10 Crystal structure (XRD Analysis)

XRD patterns of CeO_2 substituted $(Ba_{1-x-y}\ Ca_x\ Ce_y)\ (Zr_{0.1}\ Ti_{0.9})\ O_3$ ceramics measured at room temperature is shown in figure 31. All ceramics show pure perovskite structure and no other impurity phase was found within the XRD detection limit. To survey the phase evolution, enlarged view of peaks is shown in figure 31 (b) between 44° - 46°. For sample x;Ca = 0.05 (~ 0.80BZT-0.20BCT) peak (002) intensity is higher than the (200) peak suggesting an orthorhombic phase [43, 44]. As the Ca content increased to 0.10 (0.66BZT- 0.34BCT), the (002) peak intensity is levelling with the intensity of (200) peak which indicate either orthorhombic or orthorhombic-tetragonal phase coexistence [44]. However, when Ca content further increased to 0.15 (0.50BZT – 0.50BCZT) and 0.20 (0.30BZT – 0.70BCT) peak (002) intensity gets smaller than (200) peak suggesting a single tetragonal phase. Similar results were discovered previously [45 – 47]. Therefore, we conclude that there should be a phase transition (orthorhombic to tetragonal) between 0.66BZT- 0.34BCT (x;Ca=0.10) and 0.50BZT – 0.50BCZT (x;Ca=0.15) composition which is believed to be a phase convergence region (MPB). This explanation is in agreement with the previous report [35]. Single rhombohedral phase was found below 0.68BZT-0.32BCT composition while C-R-T triple point was found for 0.50BZT-0.50BCT composition by Lui and Ren [12] however, Keeble et.al [35] modified this phase diagram by an introduction of bridging orthorhombic phase near 0.50BZT-0.50BCT which is found to be valid in our case. Also, the peak shift towards higher angles has been also observed near 45° which indicate cell contraction. This observation is consistent with the cerium incorporation at A site of perovskite structure.

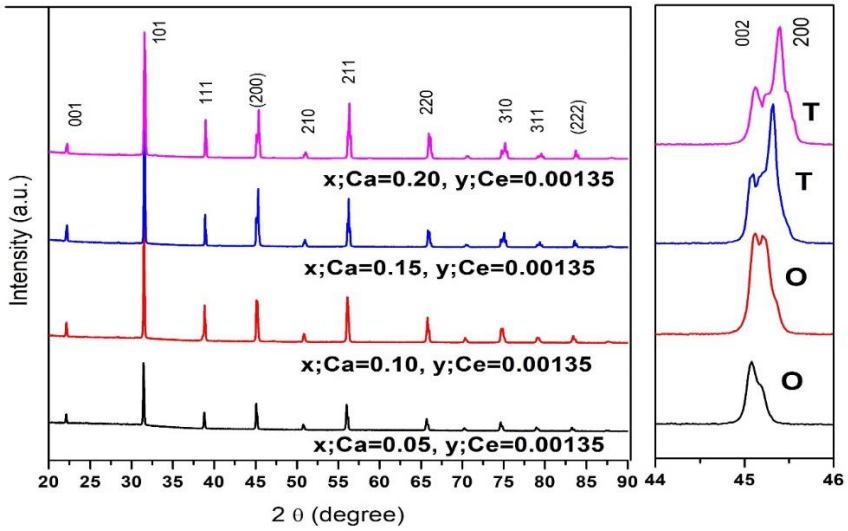

Fig. 31 X ray diffraction patterns of $(Ba_{1-x-y}\ Ca_x\ Ce_y)\ (Zr_{0.1}\ Ti_{0.9})\ O_3$ ceramics sintered at 1425 °C/4h

(V) B-site substitution of CeO_2: Synthesis and characterization of $(Ba_{0.85}\ Ca_{0.15})\ (Zr_w\ Ce_y\ Ti_{1-w-y})\ O_3$ ceramics

$(Ba_{0.85}\ Ca_{0.15})\ (Zr_w\ Ce_y\ Ti_{1-w-y})\ O_3$ ceramics where, w;Zr = 0, 0.05, 0.1, 0.2 moles and y;Ce = 0.00135 mol. prepared by solid state reaction route. The corresponding Ti content were 0.99, 0.94, 0.89 and 0.79. These Zr, Ti and Ce ratios in the $(Ba_{0.85}\ Ca_{0.15})\ (Zr_w\ Ce_y\ Ti_{1-w-y})\ O_3$ composition are very close to 0BZT-0.99BCT, 0.20BZT-0.75BCT, 0.50BZT-0.50BCT and 0.99BZT-0.1BCT compositions. Again, we fixed y;Ce content as 0.00135 at which, we obtained high piezoelectric properties described in section 6 II. The reason of taking this composition into account is to see the effect of Ce on B-site as well as on structure, microstructure and functional properties of BCZT ceramics with changing Zr and Ti ratios.

4.11 Microstructures and density

Figure 32 shows SEM observations of these ceramics sintered at 1400 °C for 4 hours. With increasing Zr (x mol.) average grain size increased from ~ 12 um (x = 0) to ~ 22 um (x = 0.2). These results show the microstructure evolution of these ceramics. All samples are dense enough except few small porosities. Other reports [46] also shown that the morphology of $Ba(ZrTi)O_3$ materials strongly dependent on Zr content and it helps to improve the grain growth of these materials.

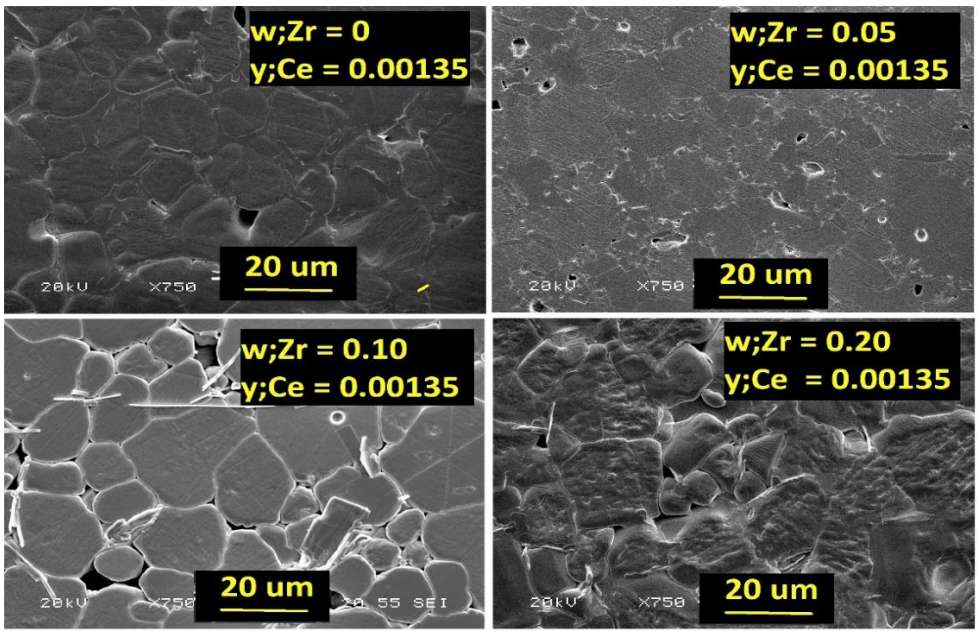

Fig. 32 Microstructures of $(Ba_{0.85}\ Ca_{0.15})\ (Zr_w\ Ce_y\ Ti_{1-w-y})\ O_3$ ceramics sintered at 1400 °C/4h

4.12 Functional properties

Figure 33 and 34 depicts piezoelectric properties (d_{33} & k_p) of these ceramics at different sintering temperatures. d_{33} first increases as the sintering temperature increases and then decreases. k_p follows the same trend. Peak values of d_{33} and k_p were obtained for w;Zr = 0.1 as 361 ±10 pC/N and 42.8± 1, respectively, at 1400°C.

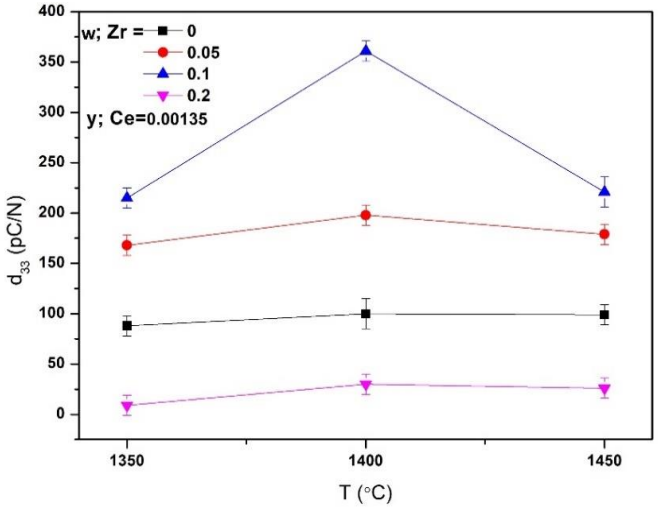

Fig. 33 Piezoelectric constant of $(Ba_{0.85}\ Ca_{0.15})\ (Zr_w\ Ce_y\ Ti_{1-w-y})\ O_3$ ceramics sintered at different temperatures

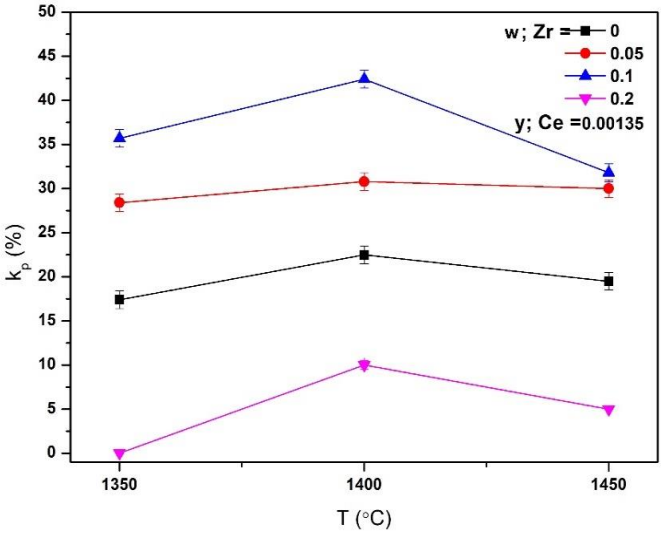

Fig. 34 Planar coupling constants of $(Ba_{0.85}\ Ca_{0.15})\ (Zr_w\ Ce_y\ Ti_{1-w-y})\ O_3$ ceramics sintered at different temperatures

Figure 35 shows relative permittivity and dielectric loss as a function Zr content for $(Ba_{0.85}\ Ca_{0.15})\ (Zr_x\ Ce_y\ Ti_{1-x-y})\ O_3$ ceramics sintered at 1400 °C/4h. Clearly, as the Zr content increases ε_r increases

and tan δ decreases. ε_r values increased to a peak value of 5937±50 for x = 0.2. Generally, the pseudo cubic structured ceramic (here x = 0.2) exhibits higher relative permittivity than the tetragonal or orthorhombic ones [46]. It is also reported that with increase in Zr content dielectric loss is also increased [46] but here we found the opposite. It may be explained like this. This may be due to the Ce ions. However, the mechanism for the effect of CeO_2 is more complex. Ce ions possibly exist in BCZT structure in two valance states. Ce^{4+} ions in the radius of 0.087 nm, and Ce^{3+} in ionic radius of 0.101 nm. In view of the radius Ce^{3+} ions cannot enter B site of the perovskite but can occupy A site including A1 site of Ba^{2+} (0.135 nm) and A2 site of Ca^{2+} (0.1 nm). Since the ionic radius of Ce^{3+} is less than Ba^{2+} and nearly same as Ca^{2+}, therefore does not cause deformation to the BCZT lattice. While in contrast Ce^{4+} ions have smaller radius and can occupy either Zr^{4+} or Ti^{4+} site. The possible occupation of Ce^{4+} at B site cannot lead O vacancy but it may change the space charges to supress the domain movement resulting the decrease in dielectric loss (tan δ). However, to explain the decrease in dielectric loss with increasing Zr content is more complicated and one might expect increase in dielectric loss could be near the phase change irrespective of compositional changes (See also figure 36).

Figure 36 shows the temperature dependent dielectric properties of $(Ba_{0.85}\ Ca_{0.15})\ (Zr_x\ Ce_y\ Ti_{1-x-y})\ O_3$ ceramics sintered at 1400 °C/4h where w;Zr = 0, 0.05, 0.10, 0.20 and y;Ce = 0.00135. The corresponding Ti content were 0.99, 0.94, 0.89 and 0.79. These Zr, Ti and Ce ratios are very close to 0BZT-0.99BCT, 0.20BZT-0.75BCT, 0.50BZT-0.50BCT and 0.99BZT-0.1BCT compositions respectively. When w;Zr content is 0 and 0.05, only one phase transition is observed near T_C. This is in consistent with the previous reports. While as we move towards w;Zr=0.1 or 0.50BZT-0.50BCT composition, the two obvious peaks are observed corresponding to T_{R-O} and T_{O-T} phase transitions. For further increment in Zr content (w = 0.2), a single broad peak is observed which suggests that tetragonal and cubic phase transitions are very close to each other which shifted the peak near room temperature. It is well known that room temperature relative permittivity abruptly increases when phase transition point is close to the room temperature [46]. This behaviour is valid for the sample w;Zr = 0.2. Also, it should be noted that the T_C is found >120°C for w:Zr = 0, 0.05 while further increase in Zr content (w=0.1) gradually reduced to 100°C. Addition of w:Zr = 0.2, the T_C drastically deteriorated. Therefore, it is concluded that, T_C could be tailored with different amount of Zr content.

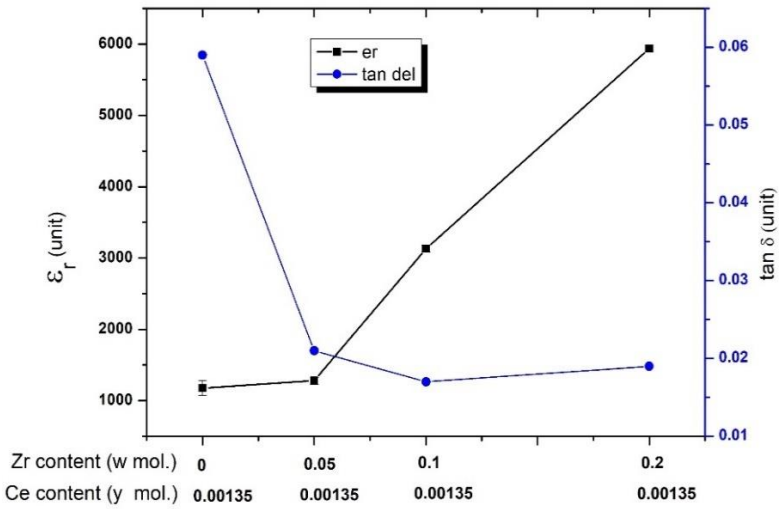

Fig. 35 Room temperature of Relative permittivity and dielectric loss of $(Ba_{0.85}\ Ca_{0.15})\ (Zr_w\ Ce_y\ Ti_{1-w-y})\ O_3$ ceramics sintered at 1400 °C/4h

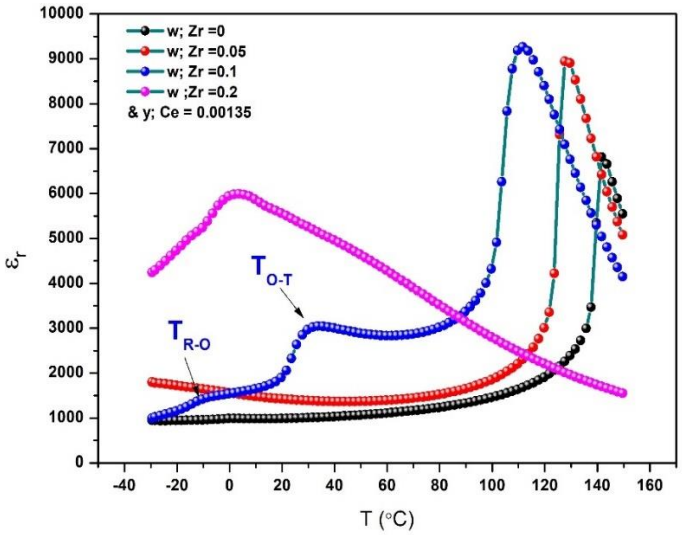

Fig. 36 ε_r -T plot of $(Ba_{0.85}\ Ca_{0.15})\ (Zr_w\ Ce_y\ Ti_{1-w-y})\ O_3$ ceramics sintered at 1400 °C/4h

Figure 37 shows the hysteresis loop (P versus E) of these ceramics with various Zr contents. The Zr content was found to have an obvious effect on the ferroelectric properties of $(Ba_{0.85}\ Ca_{0.15})\ (Zr_w\ Ce_y\ Ti_{1-w-y})\ O_3$ ceramics. The remenant polarization increases gradually from 7.43 μC/cm² to 11.30 μC/cm² with increasing x from 0 to 0.1 and then decreases sharply to 1.23 μC/cm² for x = 0.2. This might be due to the structural change. When structure changes from tetragonal to tetragonal-orthorhombic the P_r values increases. However, for pseudo cubic structure the value of P_r is very small. Also, when Zr content increases to 0.1, E_C decreases, and more square hysteresis loop is observed which indicates more internal polarizability and strain. For x = 0.2 P-E hysteresis is very weak and is associated with the excessive Zr content which lead to structural deformation.

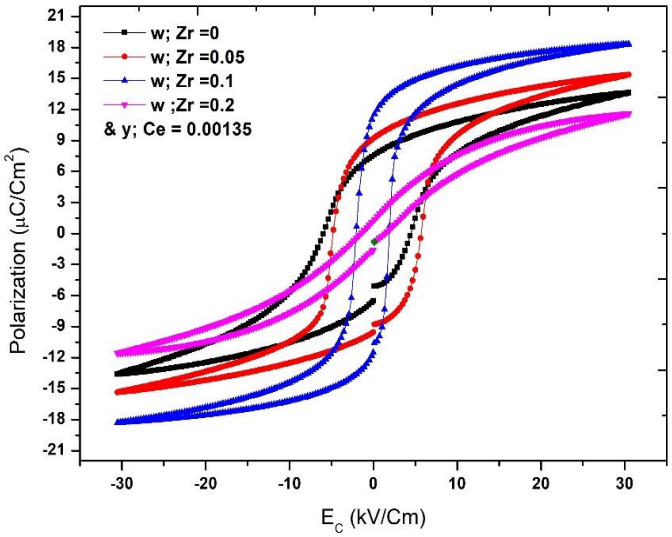

Fig. 37 P -E hysteresis plot of $(Ba_{0.85}\ Ca_{0.15})\ (Zr_x\ Ce_y\ Ti_{1-x-y})\ O_3$ ceramics sintered at 1400 °C/4h

5. Conclusion

In this thesis, processing of BCZT-Ce piezoelectric materials for advanced applications and/or basic research was shown. The main purpose of the thesis was to study the effect of cerium on BCZT ceramics due to its +3 and +4 valances with different ionic radii on the structural, microstructural and functional properties of these ceramics. In this way Ce was used as an additive as well as substitutive at A and B site of BCZT perovskite structure. The main points are as follows:

- When Ce is used as an additive, pure perovskite structure is formed in which no secondary or impurity phase was observed. Both XRD analysis and Raman spectra suggested the coexistence of rhombohedral-tetragonal (R-T) phases, when Ce is used as an additive in the range y = 0 - 0.1 wt.%. This phase coexistence is an indication of morphotropic phase boundary where functional properties could be enhanced. From XRD and Raman spectra, there was no clear indication of Ce ions occupation of different sites. However, E_C has been lowered due to the Ce addition which might be an indication of soft nature of these ceramics and therefore we speculate Ce ions occupation at A site.

- It is noted that temperature and grain size play an important role in achieving high functional properties but at the same time, the amount of CeO_2 can also affect the sinterability and densities of BCZT ceramics. Therefore, one need to be bit more careful about the proper amount of CeO_2 incorporation. The sintering temperature has been reduced to 1350 °C which is almost 200 °C sintering temperature reduction in achieving very high functional properties. Two step sintering technique is a useful technique while reducing grain sizes and obtaining highly dense microstructures but for BCZT-Ce ceramics. It is noted that, grain sizes less than 10 μm may lead to a deterioration in piezoelectric properties.

- When CeO_2 (y = 0 - 0.02 mol.) used as a substitute at A site of $(Ba_{0.85}Ca_{0.15-y}Ce_y)(Zr_{0.1}Ti_{0.9})O_3$ ceramics, XRD analysis show peak shift towards higher angles which clearly suggest cell contraction and therefore, we conclude that the Ce ions may occupy A site. Raman spectra confirms the R-T phase coexistence in the range y = 0 - 0.00135. It is found that 10 - 13 µm grain size is critical for obtaining high piezoelectric properties (d_{33} > 500 pC/N) for y = 0.00135.

- To investigate further, $(Ba_{1-x-y}Ca_xCe_y)(Zr_{0.1}Ti_{0.9})O_3$ was prepared where x;Ca = 0.05, 0.10, 0.15, 0.02 & y;Ce = 0.00135. Again, high d_{33} ~ 457 pC/N is obtained with ~ 13 µm grain size samples and better density at for samples sintered at 1425 °C/4h. The little decrease in d_{33} is may be due to the change in Ba and Ca compositional ratios. Here also, XRD analysis confirms the occupation of Ce ions at A site due to the contraction in the primitive cell. It is also concluded that with increase in Ca content the phase transition may occur from orthorhombic to tetragonal which might affect the properties of these ceramics.

- $(Ba_{0.85}Ca_{0.15})(Zr_wCe_yTi_{1-w-y})O_3$ ceramics where w;Zr = 0, 0.05, 0.10, 0.20 & y;Ce = 0.00135 were prepared. XRD analysis shows a coexistence of tetragonal and orthorhombic phases for Zr (w) = 0.1 and Ce (y) = 0.00135. Temperature dependent dielectric properties show that as the Zr content increases up to 0.1, the T_{O-T} and T_{R-O} peaks appeared. Excess of Zr content shifts the T_{T-C} peak to very low temperature that can severe piezoelectric properties. Ferroelectric properties also shown dependence on the structural change of these ceramics. The better P_r values may be obtained for orthorhombic - tetragonal structure.

- Therefore, based on above research, addition of 0.07 wt.% CeO2 to $(Ba_{0.85}Ca_{0.15})(Zr_{0.1}Ti_{0.9})O_3$ after calcination at 1250°C/2h would give high piezoelectric properties (d33 > 500 pC/N) with density over 96% (of t.d.) while sintering temperature can be reduced down to 1350°C/4h. Similarly, when Ce=0.00135 mol. is substituted at A site of $(Ba_{0.85}Ca_{0.15-y}Ce_y)(Zr_{0.1}Ti_{0.9})O_3$ceramics and calcined together with CeO_2 at 1250°C/2h, similar high d33 (~ 500 pC/N) could be achieved at low sintering temperature 1350°C/4h.

- In this thesis work, BCZT- yCeO2 (y = 0 – 3 wt.%) ceramics were successfully prepared and effect of Ce on BCZT ceramics on structure, microstructures and functional properties was demonstrated with range of sintering temperature. Then Ce used as a substitution at A and B site of BCZT perovskite structure and results were compared to the results obtained from Ce addition to the BCZT ceramics. It is found that Ce addition (y = 0.07 wt.%) and Ce substitution at A site (0.00135 mol.) may reduce sintering temperature to 1350°C with high piezoelectric properties (d_{33} ~ 500pC/N).

6. Future Work

- In this thesis, effect of range of Ce doping (y = 0 – 3 wt.%) on BCZT ceramics is presented in section 6(I). The correlation between structure, microstructure and its functional properties were studied. However, microstructure evolution for the samples > 0.1 wt.% at range of sintering temperature was not clear. For this, HRTEM would be used. In addition, y = 1 wt.% sample show anomalous behaviour throughout which might guide the synthesis process of these ceramics.
- Rietveld refinement need to be done in order to understand the crystal symmetry and phase transitions. Also, in Section 6 (V), to understand Ce^{4+} ions occupation at B site is more complex so there need to calculate lattice distortions and change in lattice parameters in order to understand the Ce^{4+} occupation at B-site. For this Rietveld refinement may help.
- For composition $(Ba_{0.85}\ Ca_{0.15})\ (Zr_w\ Ce_y\ Ti_{1-w-y})\ O_3$, the Curie temperature were observed between 100°C – 140°C with different Zr content (Section 6V). More compositional optimization need to be done in order to enhance the Curie temperature of $(Ba_{0.85}\ Ca_{0.15})\ (Zr_w\ Ce_y\ Ti_{1-w-y})\ O_3$ ceramics. This would promote such lead free materials to substitute traditional lead based materials for wider applications. Also, this issue could be resolved by introducing compositions with much higher curie temperature such as KNN, and $BiFeO_3$ etc.
- The sintering temperature of BCZT ceramic is reduced to 1350°C by CeO_2 addition while maintaining high piezoelectric properties. Further reduction in sintering temperature could be done by the help of co-doping of CeO_2 as an addition and Li_2CO_3 as a sintering aid for its industrial transfer.

7. Selected References

[1] Y Saito, H Takao, T Tani, T Nonoyama, K Takatori, T Homma, T Nagaya, M Nakamura. Lead free piezoceramics, Nature, vol. 7. p84-87, 2004.

[2] EU-Directive 2002/96/EC: Waste Electrical and Electronic Equipment (WEEE). Office Journal of European Union. vol. 46, pp. 24-38, 2003.

[3] Union, EU-Directive 2002/95/EC: Restriction of the Use of Certain Hazardous Substances in Electrical and Electronic Equipment (RoHS). Office Journal of the European. Vol.46, pp.19-23, 2003.

[4] EU-Commission Directive 2000/71/EC Official Journal of the European Communities L287 pp.46–50., 2000.

[5] J Wook , D Robert, M Acosta, J Zang, C Groh, E Sapper, K Wang, J Rödel. Giant electric-field-induced strains in lead-free ceramics for actuator applications – status and perspective, J. Electrocer. vol. 29, pp.71–93, 2012.

[6] M Demartin, D Damjanovic, N Setter. Lead Free Piezoelectric Materials, J. Electrocer. vol. 13, pp. 385–392, 2004.

[7] T Shrout, S Zhang. lead free piezoelectric ceramics, J. Electrocer. vol. 19, pp. 113–26, 2007.

[8] J Li and K Wang, Ferroelectric and Piezoelectric Properties of Fine-Grained $Na_{0.5}K_{0.5}NbO_3$ Lead-Free Piezoelectric Ceramics Prepared by Spark Plasma Sintering. J. Am. Ceram. Soc, vol. 89, pp.706–09, 2006.

[9] J Rodel, W Jo, KTP Seifert, EM Anton, T Granzow, D Damjanovic. Perspective on the development of lead-free piezoceramics. J. Am. Ceram. Soc., vol. 92, pp. 1153–77, 2009.

[10] PK Panda, Review: environmental friendly lead-free piezoelectric materials, J. Mater Sci. vol. 44, pp.5049–62, 2010.

[11] E Aksel, JL Jones. Advances in lead free piezoelectric materials for sensors and actuators, Sensors vol. 10, pp. 1935–54, 2010.

[12] W Liu, X Ren. Large piezoelectric effect in Pb-free ceramics, Phys. Rev. Lett. , vol. 103, 257602, 2009.

[13] A Reyes -Montero, L Pardo, R López -Juárez, A M González, S O Rea- López, M P Cruz and M E Villafuerte-Castrejón. Sub-10μm grain size, $Ba_{1-x}Ca_xTi_{0.9}Zr_{0.1}O_3$ (x = 0.10 and x = 0.15) piezoceramics processed using a reduced thermal treatment. Smart Mater. Struct., vol. 24, 065033, 2015.

[14] M Jiang, Q Lin, D Lin, Q Zheng, X Fan, X Wu, H Sun, Y Wan, Y Wu. Effects of MnO_2 and sintering temperature on microstructure, ferroelectric, and piezoelectric properties of $Ba_{0.85}Ca_{0.15}Ti_{0.9}Zr_{0.1}O_3$ lead-free ceramics. J. Mater. Sci., vol. 48, pp.1035–1041, 2013.

[15] Y Cui, X Liu, M Jiang, X Zhao, X Shan, W Li, C Yuan, C Zhou. Lead-free $Ba_{0.85}Ca_{0.15}Ti_{0.9}Zr_{0.1}O_3$-$CeO_2$ ceramics with high piezoelectric coefficient obtained by low-temperature sintering. Ceram. Int., vol. 38, pp. 4761–4764, 2012.

[16] K Castkova, K Maca, J Cihlar, H Hughes, A Matousek, P Tofel, Y Bai, and TW Button. Chemical Synthesis, Sintering and Piezoelectric Properties of $Ba_{0.85}Ca_{0.15}Zr_{0.1}Ti_{0.9}O_3$ Lead-Free Ceramics. J. Am. Ceram. Soc., vol. 98, pp. 2373–2380, 2015

[17] Suk-Joong, L. Kang. Sintering, densification, grain growth and microstructure. Elsevier Butterworth-Heinemann publication, Vol. 9, pp.89-135, 2005.

[18] Y Bai, A Matousek, P Tofel, V Bijalwan, B Nan, H Hughes, TW Button. (Ba,Ca)(Zr,Ti)O_3 lead-free piezoelectric ceramics—The critical role ofprocessing on properties. Jr. of Eur. Ceram. Soc., vol. 35, pp. 3445–3456, 2015.

[19] D Gao, KW Kwok, D Lin, HLW Chan. Microstructure, electrical properties of CeO_2-doped $(K_{0.5}Na_{0.5})NbO_3$ lead-free piezoelectric ceramics. J. Mater Sci. vol.44 , pp.2466–2470, 2009.

[20] J Hao, W Bai, W Li, J Zhai. Correlation Between the Microstructure and Electrical Properties in High-Performance $(Ba_{0.85}Ca_{0.15})$ $(Zr_{0.1}Ti_{0.9})$ O_3 Lead-Free Piezoelectric Ceramics. J. Am. Ceram. Soc., vol. 95, pp. 1998–2006, 2012.

[21] H. L. Sun, Q. J. Zhen, Y Wan, Y Chen, X Wu, K W. Kwok, H. L. W. Chan, D. M. Lin. Correlation of grain size, phase transition and piezoelectric properties in $Ba_{0.85}Ca_{0.15}Ti_{0.90}Zr_{0.10}O_3$ ceramics. J Mater Sci: Mater. Electr. vol. 26, pp.5270–5278, 2015.

[22] L Zhang, M Zhang, L Wang, C Zhou, Z Zhang, Y Yao, L Zhang, D Xue, X Lou, and X Ren. Phase transitions and the piezoelectricity around morphotropic phase boundary in $Ba(Zr_{0.2}Ti_{0.8})O_3$-$x(Ba_{0.7}Ca_{0.3})TiO_3$ lead-free solid solutions. Appl. Phy. Lett. vol. 105, 162908, 2014.

[23] JC Burfoot, H T Martirena. Grain-Size Effects on Properties of Some Ferroelectric Ceramics. J. Phys. C: Solid State Phys, vol. 7, pp.3182–3192, 1974.

[24] M. H. Frey and D. A. Payne. Grain-Size Effect on Structure and Phase Transformations for Barium Titanate. Phys. Rev. B, vol. 54, pp.3158–67, 1996.

[25] R Hayati, MA Bahrevar, T Ebadzadeh, V Rojas, N Novak, J Koruza. Effects of Bi2O3 additive on sintering process and dielectric, ferroelectric, and piezoelectric properties of $Ba_{0.85}Ca_{0.15}Ti_{0.9}Zr_{0.1}O_3$ lead free poiezoelectric ceramics. Jr. of Eur. Ceram. Soc., vol.36, pp.3391–3400, 2016.

[26] L Zhang, WL Zhong, YG Wang, PL Zhang. The Cell volume Effect in Barium Strontium Titanate. Sol. State Commun. vol 104, pp.263–266, 1997.

[27] K Uchino, S Nomura. Critical exponents of the dielectric constants in diffused-phase-transition crystals. Ferroelec., vol. 44, pp.55-61, 1982.

[28] A B Haugen, J S. Forrester, D Damjanovic, B Li, K J Bowman, and J L Jones· Structure and phase transitions in 0.5(Ba0.7Ca0.3TiO3) - 0.5(BaZr0.2Ti0.8O3) from –100°C to 150°C. J. Appl. Phys. vol.113, 014103, 2013.

[29] M. C. Ehmke, S. N. Ehrlich, J. E. Blendell, and K. J. Bowman. Phase Coexistence and Ferroelastic Texture in High Strain (1-x)$Ba(Zr_{0.2}Ti_{0.8})O_3$– $(Ba_{0.7}Ca_{0.3})TiO_3$ Piezoceramics. J. Appl. Phys. vol 111,[2], 124110, 2011.

[30] R sasaki, R Suzuki, S Uraki, H Kakimoto, T Tsurumi. Low temperature sintering of alkaline niobate based piezoelectric ceramics using sintering aids. J. of ceram. Soc. of Jap. Vol. 116, pp.1182-1186, 2008.

[31] Y Tsur, T D Dunbar, C A Randall. Crystal and Defect Chemistry of Rare Earth Cations in $BaTiO_3$. J. Electroceram. vol. 7, pp.25-35, 2001.

[32] W Li, Z Xu, R Chu, P Fu, G Zang. Temperature stability in Dy-doped $(Ba_{0.99}Ca_{0.01})$ $(Ti_{0.98}Zr_{0.02})$ O_3 lead-free ceramics with high piezoelectric coefficient. J. Am. Ceram. Soc. vol.94, pp.3181–3183, 2011.

[33] R.D. Shannon. Revised Effective Ionic Radii and Systematic Studies of Interatomic Distances in Halides and Chalcogenides, Acta Cryst. vol. A32, 751-767, 1976.

[34] D. Makovec, Z. Samardzija, and D. Kolar. Solid Solubility of Cerium in $BaTiO_3$. J sol. state chem., vol.123, pp.30–38, 1996.

[35] DS. Keeble, F Benabdallah, PA. Thomas, M Maglione, J Kreisel. Revised structural phase diagram of $(Ba_{0.7}Ca_{0.3}TiO_3)$-$(BaZr_{0.2}Ti_{0.8}O_3)$. Appl. Phy. Lett., vol. 102, 092903, 2013.

[36] Miao S, Pokorny J, Pasha UM, Thakur OP, Sinclair DC, Reaney IM, Polar order and diffuse scatter in $Ba(Ti_{1-x}Zr_x)O_3$ ceramics. J Appl Phys.vol. 106 (11):114111, 2009.

[37] M Deluca, L Stoleriu, L Curecheriu, N Horchidan, A Ianculescu, C Galassi and L Mitoseriu. High-field dielectric properties and Raman spectroscopic investi-gation of the ferroelectric-to-relaxor crossover in $BaSn_xTi_{1-x}O_3$ ceramics. J Appl Phys, vol.111(8):08410217, 2012.

[38] L Zhao, B Zhang, P Zhou, L Zhu, J Li. Effect of Li_2O addition on sintering and piezoelectric propertiesof (Ba,Ca)(Ti,Sn)O3lead-free piezoceramics. J. Eur. Ceram. Soc , vol. 35, pp.533–540, 2015.

[39] Dobal PS, Katiyar RS. Studies on ferroelectric perovskites and Bi-layered compounds using micro-Raman spectroscopy. J Raman Spectrosc, vol. 33(6), pp.405–423, 2002.

[40] Farhi R, ElMarssi M, Simon A, Ravez J. A Raman and dielectric study offerroelectric $Ba(Ti_{1-x}Zr_x)O_3$ ceramics. Eur Phys. Jr. B , 1999, vol. 9(4), pp.599–604, 1999.

[41] J Shia, W Yanga. Piezoelectric and dielectric properties of CeO_2-doped $(Bi_{0.5}Na_{0.5})_{0.94}Ba_{0.06}TiO_3$ lead-free ceramics. J. All. Com. vol. 472, pp.267–270, 2009.

[42] H Orihara, S Hashimoto, and Y Ishibashi. A Theory of D-E Hysteresis Loop Based on the Avrami Model. Journal of Physical Society of Japan, vol. 63, pp.1031-1035, 1994.

[43] L Zhu, B Zhang, L Shun Li, Y Zhou, X Shi, N Wang. Large piezoelectric effect of $(Ba,Ca)TiO_3–xBa(Sn,Ti)O_3$ lead-free ceramics. J. Eur. Ceram. Soc., vol. 36, pp.1017–1024, 2016.

[44] X Chao, J Wang, J Pu, S Zhang, Z Yang. Aging behavior and electrical properties of low-temperature sintered (Ba, Ca)(Ti, Zr)O3-Ba(Cu, W)O3ceramics and plate loudspeaker. Sensors and Actuators, vol. A 237, pp.9–19, 2016.

[45] J Wu, A Habibul, X Cheng, X Wang, B Zhang. Orthorhombic–tetragonal phase coexistence and piezoelectric behavior in $(1–x)(Ba,Ca)(Ti,Sn)O_3–x(Ba,Ca)(Ti,Zr)O_3$ lead-free ceramics. Mat. Res. Bull., vol. 48, pp.4411–4414, 2013.

[46] S Zhang, H Zhang, B Zhang, S Yang. Phase-transition behavior and piezoelectric properties of lead-free $(Ba_{0.95}Ca_{0.05})(Ti_{1-x}Zr_x)O_3$ ceramics. J. All. Com., vol.506, pp.131–135, 2010.

[47] X Wang, P Liang, L Wei, X Chao, Z Yang. Phase evolution and enhanced electrical properties of $(Ba_{0.85Ca}0.15_{2x}Y_x)(Zr_{0.1}Ti_{0.9})O_3$ lead-free ceramics. J Mater Sci: Mater Electron, vol.26, pp.5217–5225, 2015.

8.Summary of Author's activities:

Publications:

- $(Ba,Ca)(Zr,Ti)O_3$ lead-free piezoelectric ceramics- The critical role of processing on properties Yang Bai, Ales Matousek, Pavel Tofel, **Vijay Bijalwan**, Bo Nan, Hana Hughes, Tim W. Button. Journal of the European Ceramic Society, 35, 3445–3456,2015

- IEEE Conference paper- Phase Transitions and Dielectric, Ferroelectric and Piezoelectric Properties of $Bi_{0.5}(Na_{0.82}K_{0.18})_{0.5}TiO_3$-Doped $(Ba_{0.85}Ca_{0.15})$ $(Zr_{0.1}Ti_{0.9})O_3$ Ceramics, Yang Bai, Ales Matousek, Pavel Tofel, Bo Nan, **Vijay Bijalwan**, Michael Kral, Hojat Pooladvand, Hana Hughes and Tim W. Button, IEEE conference Singapore, 268 – 271, 2015

- The effect of sintering temperature on the ferroelectric, dielectric and piezoelectric properties of BCZT-$xCeO_2$ lead free ceramics. **Vijay Bijalwan**, Hana Hughes, Hojat Pooladvand, Pavel Tofel, Yang Bai, Bo Nan, Ales Matousek, Vladimir Holcman and Tim W. Button. Manuscript submitted to Journal of American ceramic society.

- The complex evaluation of piezoelectric properties of nearly dense BCZT ceramic in dependence on its grain size. **Vijay Bijalwan**, Pavel Tofel, Jiří Erhart, Karel Maca. Manuscript submitted to ceramic international journal.

- Grain size dependence of microstructure and functional properties of $(Ba_{0.85}\ Ca_{0.15-x}\ Ce_x)(Zr_{0.1}\ Ti_{0.9})\ O_3$ lead free piezoelectric ceramics. **Vijay Bijalwan**, Pavel Tofel, Vladimir Holcman. Manuscript submitted to Journal of Asian ceramic societies.

Participation in research projects:

- GACR P108-13-09967S "A fundamental study of the effect of synthesis and processing conditions on the structure and properties of $(Ba,Ca)(Ti,Zr)O_3$ lead-free piezoceramics", coordinator- Prof. Tim Button, 2014-2015

- Project STI-J-15-2900, CEITEC BUT "Fabrication of Multi-Layer Actuators with Lead-free Piezoelectric Compositions" coordinators- Prof. Tim Button, Dr. Yang Bai, 2016

- GACR 18-20498S "Control of microstructure and properties of lead-free piezoceramic materials through advanced ceramic processing", coordinators- Prof. Karel Maca, Prof. Jiří Erhart- Ongoing project

Internships and training/Other activities:

- University of Aveiro, Portugal. September 2015 (2 weeks)
- School of metallurgy and materials, University of Birmingham, United Kingdom. Jan-June 2016 (6 months)
- Training and supervised undergraduate students for their bachelor's and master thesis.